RESEARCH AND DEVELOPMENT BRANCH
DEPARTMENT OF NATIONAL DEFENCE
CANADA

DEFENCE RESEARCH ESTABLISHMENT OTTAWA

DREO REPORT NO. 709
DREO R 709

NEAR-SURFACE CURRENT IN ROBESON CHANNEL

by

R.K. Chow

PROJECT NO.
97-67-05

JANUARY 1975
OTTAWA

array being intended to gather data from the latter part of April to the early part of June. The station in the middle of the channel was first occupied as a base camp for the semi-permanent field party stationed on the ice (Station No. 2 of Figure 2). After the installation of the instruments at this station, the field party was to travel by skidoo to deploy instruments at Station No. 1 (near Ellesmere Island) and at Station No. 3 (near Greenland) and to remain on the ice to gather atmospheric and other environmental data until the recovery of the current meters.

Figure 3 depicts schematically the arrays of current meters at the three stations. It was believed that the near-surface current profile in the middle of the channel was more important than that at the other stations. For this reason, five of a total of seven current meters were installed at Station No. 2 at depths of 2.25, 7.25, 20, 50 and 75 m below the ice. Each of the remaining stations had only one current meter at a depth of 50 m. As will be seen later from the results, a better arrangement of the meters would have been achieved by having more meters at the station closest to Ellesmere Island (Station No. 1) since the current velocity was found to decrease across the channel from Ellesmere Island to Greenland and for the same depth the current seems to be more dramatic and intense on the Ellesmere side of the channel.

Installation Method

During this operation, the mooring and the recovery of the instruments were done manually without the aid of a winch. For this reason, it was desirable to have only one or two meters per mooring in Station No. 2 in order to keep the weight of each mooring to a minimum for easy handling. Another advantage to such an arrangement is that, in the event of a cable break, the number of instruments lost is limited to the one or two meters on the string rather than the whole station. Four moorings were used for the five meters in Station No. 2 with two shallow meters in one string and each of the deeper ones having its own mooring. The lateral separation between adjacent moorings for this station was about 100 m to avoid the entangling of the cables.

The sampling times (Δt) of the current meters were not all the same. For the six meters at Stations No. 1 and 2, Δt was set at 60 minutes while for the remaining meter at Station No. 3, it was set for 20 minutes. This shorter sampling time was chosen later because it was felt that perhaps some future studies might require the consideration of phenomena with frequencies higher than 1/2 cph (the so-called Nyquist frequency limit for the one-hour sampling time).

No further account of the deployment of the instruments will be given here as an extensive account of the equipment, preparation of holes through the ice as well as mooring procedure can be found in a previous technical note by Finlayson[3].

Operational Problems

The study of the near-surface current was hampered in several ways. After the installation of Station No. 2, it was realized that the manoeuverability of the field party was greatly restricted by the rough ice in the channel so that the original aim of dividing the channel into four approximately equal segments had to be abandoned. The distances between neighbouring stations were small in comparison with the channel width of about 30 km, the separations between Stations No. 1 and 2 and between Stations No. 2 and 3 being only approximately 3.7 and 1.7 km, respectively. Consequently the area spanned by the meters was confined to a small region in the cross section of the channel. Four of the seven meters stopped registering the current speed after some period of operation (although the current direction was recorded faithfully). Moreover, Station 3, with one of the remaining three meters, could not be deployed until about two weeks before the recovery of all meters so that the record length for this station was relatively short - about 15 days. Thus, of the seven meters, only two yielded continuous records for the whole period of deployment. The record lengths of the other five meters were much shorter than desirable

Data Reading

The Braincon meter records data in analog form on 16 mm photographic films. These were then processed into digital form by a well-established procedure at the Bedford Institute of Oceanography. After this initial reduction the current velocity in the form of speed and direction relative to true north can be easily obtained. These two quantities will be represented by V and ϕ, respectively, in subsequent discussion.

METHODS OF ANALYSIS

Ocean currents are vector quantities varying with space and with time. Our notation will be such that a current velocity $\vec{V}(\vec{r},t)$ will denote the velocity $\vec{V}$ at time t at the point $\vec{r}$ in a body of water. Frequently, either or both of the space-time variables will be omitted for brevity. Thus, in the next section on the component representation of currents, it is convenient to drop both dependent variables. However, in the discussion the Fourier transform in which integration is performed over the time domain, only the temporal variable is kept, e.g. $\vec{V}(t)$, with $\vec{r}$ understood to be the coordinate point in the body of the water in question. Since the current is sampled at a discrete time interval Δt for a finite duration $T = (N-1)\Delta t$, we introduce a further notation of $\vec{V}(t_k)$ to denote the current velocity at time $t_k = k\Delta t$ with the integer k in the range $o \leq k \leq N - 1$.

Component Representation of Currents

Instead of the speed and the direction of the current, it is frequently more convenient to work with the current components in vector addition and subtraction. The velocity components are particularly suitable for power spectrum analysis as each component can be analysed independently of the other.

A horizontal system of coordinates is chosen with the "major-axis" points in a "down-channel" direction (230^{o} clockwise from true north) and "minor-axis" points in a cross-channel direction (320^{o}) towards Ellesmere Island. This system of axes is illustrated at the lower left portion of Figure 2. Along these two axes any horizontal current velocity can be resolved into major and minor components which can be plotted and examined separately. Thus if one considers a current velocity at some time to be $\vec{V} = (V, \phi)$, where V is the speed and ϕ the angle of the velocity vector relative to the true north direction measured in the clockwise sense, the major and minor components of the velocity along the two axes are then

$$u = - V \cos (\phi - 50^{o}) \qquad (1a)$$

and

$$v = - V \sin (\phi - 50^{o}) , \qquad (1b)$$

respectively.

Virtual Displacement and Mass Transport

Let $\vec{V}_k$ be the average current velocity at a given location in a body of water that persisted for the time interval $k\Delta t < t < (k+1)\Delta t$. The displacement of a water parcel between time $t = k\Delta t$ and $t = (k+1)\Delta t$ is approximately given by $\vec{V}_k \Delta t$. Now suppose that the observed velocity is characteristic of an extended part of the water body. Then the displacement of a parcel of water from its initial position at t = o is given by the sum of the successive displacements at each Δt[4],

$$\vec{R}_n = \sum_{k=o}^{n} \vec{V}_k \Delta t$$

$$= \Delta t \sum_{k=o}^{n} \vec{V}_k \qquad o < n < N - 1 . \qquad (2)$$

The sequence of vectors $\vec{R}_o, \vec{R}_1, \ldots, \vec{R}_{N-1}$ traces out the "position" of a water parcel at time $t = 0, \Delta t, \ldots, T$ and therefore represent the successive "displacement" of the parcel of water. Frequently these fictitious trajectories are also referred to as "progressive vectors".

The average velocity between t = o and t = $n\Delta t$ can be obtained from the direction of $\vec{R}_n$ and the magnitude of $(\vec{R}_n/n\Delta t)$. In particular, the average velocity for the duration of operation of the meter is a vector obtainable from $\vec{R}_{N-1}$. Thus the total virtual displacement $\vec{R}_{N-1}$ can be regarded as a pictorial representation of the average current velocity which is of course identical to the vector sum of the time averages of the individual components. This pictorial representation offers a convenient means of comparing velocity measurements and average velocities between different depths as well as between different stations, particularly for current measurements by meters operating for a common period of time.

Consider the transport of water mass through a cross sectional area A of the channel during time T. If ρ and $\vec{V}$ are, respectively, the density of the water and the current velocity field over A, then the total mass transport must be

$$M = \int_o^T dt \int_A \rho \vec{V} \cdot d\vec{A}$$

where $d\vec{A}$ is an element of area and the second integral of the scalar product is over the area A. The average rate of transport of water during T is

$$\frac{M}{T} = \frac{1}{T} \int_o^T dt \int_A \rho \vec{V} \cdot d\vec{A}$$

$$= \int_A \rho \left[\frac{1}{T} \int_o^T \vec{V} dt \right] \cdot d\vec{A} \qquad (3)$$

The quantity in the brackets is the average current velocity over the period T described in the preceding paragraph. Thus the average current can be regarded as being effectively responsible for the transport of water through a channel. This same quantity is also responsible for the transport of heat and salt the average rates of which can be estimated with the knowledge of the appropriate gradients.

The virtual displacement generated from the velocity vectors accentuates the low-frequency oscillations (1/2 day to several days) of the current at the expense of the ones at high frequencies. The effect of the Coriolis force can be seen from the appearance of current loops rotating in a clockwise sense in the northern hemisphere. The gradually diminishing size of these loops can be identified with the action of the frictional force. However, because of the tidal nature of the current and the boundary effects of a narrow channel in our experiment these so-called inertial currents are usually not well developed.

The virtual displacement should not be regarded as the actual trajectory of a water parcel because there may not be any water parcel near the location of the meter having such a trajectory during $0 \leq t \leq T$ and the velocity of a real water parcel may change after flowing past the position of the meter. Also, the subsequent velocity of a parcel of water after passing the location of the meter may bear no resemblance to the velocity of the parcel of water that will enter into the location to take

its place. Thus the trajectory obtained can at best be regarded as being approximate, particularly for a prolonged period of time ($T >> \Delta t$).

Power Spectrum

The procedure of Blackman and Tukey for obtaining the power spectrum from a time series was used[5,6]. In this treatment, if $x(t)$ is a continuous time signal which, in our case, will be one of the components of the current velocity, then its frequency representation is given by the Fourier transform

$$X(f) = \int_{-\infty}^{\infty} x(t) \exp(2\pi i f t)\, dt \qquad (4)$$

with the inverse transform

$$x(t) = \int_{-\infty}^{\infty} X(f) \exp(-2\pi i f t)\, df \qquad (5)$$

where $X(f)$ is the Fourier component of $x(t)$ at the frequency f and $i = \sqrt{-1}$. The limits of integration in the time domain are actually finite in any practical case since only a finite segment of the time signal is available, say $0<t<T$, where T is the duration of the measurement. The situation can be represented by setting $x(t) = 0$ for t outside the range of $(0,T)$ so that

$$X(f) \simeq \int_{o}^{T} x(t) \exp(2\pi i f t)\, dt \qquad (6)$$

The Fourier representation is not particularly helpful in analyzing the usually noise-contaminated time signal. For instance, $X(f)$ will be different if the limits of integration are changed from $(0, T)$ to $(-T/2, T/2)$. The same effect will result on $X(f)$ if $x(t)$ is phase-modulated. A quantity which is free from such phase modulation is the "power" density defined as

$$p(f) = \frac{1}{T} |X(f)|^2 \qquad (7)$$

in which the factor $\frac{1}{T}$ is introduced to make $p(f)$ relatively independent of T.

If only the sampled values of the time signal $x(t_k)$, for $t_k = 0, \Delta t, 2\Delta t, \ldots, (N-1)\Delta t = T$, are available, the integral in equation (6) is usually replaced by a finite sum, i.e.

$$X(f) \simeq \sum_{k=o}^{N-1} x(t_k) \exp(2\pi i f t_k)\, \Delta t. \qquad (8)$$

Very efficient routines such as the Fast Fourier Transform (FFT) are available to carry out the summation[7]. However, the use of FFT places certain restrictions on $x(t)$ as well as on $X(f)$. First of all, the number of data points N must be a number of radix 2, i.e. $N = 2^j$ where j is an integer. For this reason, the length of the record used for the power spectrum analysis is usually shorter than the duration of the measurement. The power density $p(f)$ obtained is folded at $f = 0$ and at

$f = f_{max} = \frac{1}{2\Delta t}$ that is, for any integer k,

$$p(f+2kf_m) = p(f), \quad 0 < f < f_m \tag{9}$$

Moreover, the resolution of the power density p(f) from FFT is limited to within a frequency interval of $\Delta f = 1/T$ with $T = 2^J \Delta t$. Thus unless T is sufficiently large, the resolution in the power spectrum can be very poor. For this reason, the lunar fortnightly component of the current is discernible only for those records of sufficient length.

To facilitate the comparison of the power density of current components at different depths and at different stations, it is more convenient to consider the "normalized power density" by introducing a normalization constant C such that

$$1 = C\int_{-\infty}^{\infty} p(f)df$$

or

$$C = 1/\int_{-\infty}^{\infty} p(f)df \tag{10}$$

and define

$$P(f) = \frac{p(f)}{\int_{-\infty}^{\infty} p(f)df} = Cp(f) \tag{11}$$

In subsequent discussion, the power density for the current component will be denoted by P(f) rather than by p(f). Of course the symmetry relation and the restriction on the resolution will hold for P(f) as well.

In the power spectra of the tide and water temperature, the power densities for the periodic fluctuations of interest can become obscured by the large dc-power which depends, respectively, on the "chart datum level" and the depth of the thermograph. To adapt the same analysis to quantities such as water level and temperature, it is convenient to subtract out the dc-component of the power and examine the following normalized quantity,

$$P(f) = \frac{p(f) - p(0)\delta(f)}{\int_{-\infty}^{\infty}[p(f) - p(0)\delta(f)]df} \tag{12}$$

where $\delta(f)$ is the Dirac δ-function. In this new power spectrum, there is no danger of the power densities at frequencies of interest being washed out by p(0) because of the predominance of the latter.

RESULTS

A summary of the pertinent information for the meters such as station number, instrument number and depth, duration of operation and number of good records is given in Table 1. Results are presented in the forms of graphs, and computer-generated plots based on the method of analyses outlined. The results for the seven meters in the three stations are given in Figures 4 - 39. Then, for the purpose of comparison between meters at different depths and at different stations, selected record lengths for various meters are chosen for more detailed discussion.

The measured current velocity is shown in the form of the current speed V and current direction ϕ (Figures 4 - 10). The histograms of the distribution of these speeds and directions then follow (Figures 11 - 17). In the speed histograms, the threshold speed for the meter (about 3 cm/sec) can be disregarded so that, for meters that malfunctioned for some period, a more meaningful interpretation can be made. The current velocity is resolved into down- and cross-channel components for further examination (Figures 18 - 24). The velocity vectors are then represented by virtual displacement vectors (Figures 25 - 31) which are convenient for the computation of the average velocity and mass transport of water through a cross section of the channel. Finally, the normalized power spectrum for each component is obtained (Figures 32 - 38). From these power spectra, the surges of the current velocity due to the diurnal and semidiurnal tidal oscillations can easily be identified. Other components of the power spectra that cannot be related to the tidal periods are later identified with internal waves at the boundary layer(s) between apparently different water masses at about 50 to 150 m.

DISCUSSION

Current Speed and Direction

From the plots of the current speed, the lunar envelope can be clearly seen. The maxima of the envelope (spring tide periods) correspond approximately to the occurrence of new and full moons and the minima to the first and last quarters. The presence of four maxima (and minima) in the current speed in a lunar day (24.83 hours) indicates that the tidal oscillations are strongly semi-diurnal in character. This is substantiated by the plot of the water level as measured by the tide gauge near the site of the current observations (Figures 39(a) and 40(a)) The maximum current is about 75 cm/sec. and this occurred at 75 m in Station 2. (The current speed of 90 cm/sec at this depth is probably spurious since it is not within the lunar envelope).*

---

* Probably an error introduced during data reading.

TABLE 1. SUMMARY OF INSTRUMENT OPERATION

Station	Water Depth (m)	Meter No.	Meter Depth (m)	Start Time (GMT)	Stop Time (GMT)	Sampling Rate (Min)	No. of Readings	Beginning of Malfunction (Approximate)	No. of Good Continuous Readings (Approximate)
I	611	237	50	May 3 2246	Jun 7 1746	60	834	None	All
II	582	322	2.25	Apr 29 1911	Jun 7 1511	60	931	May 19	750
		233	7.25	Apr 29 1902	Jun 7 1602	60	932	May 19	690
		236	20	Apr 29 2208	Jun 7 1908	60	932	May 18	430
		235	50	Apr 29 2116	Jun 7 1618	60	930	May 18	430
		234	75	Apr 25 2320	Jun 7 1420	60	1022	None	All
III	454	238	50	May 23 2110	Jun 7 1930	20	1074	None	All

The oscillation of the current speed generally increased with depth as illustrated by plots for the arrays of meters at Station 2 (Figures 5 - 9). Moreover, for the same depth at which a meter was present at each station (50 m) and for a common period of time, the oscillation for the station nearest Ellesmere Island is the largest (Figures 4, 8 and 10). No comparison between Stations 2 and 3 can be made at this depth as there was no reliable simultaneous reading due to the failure of one of the two meters. Because of the very small number of stations, it is not known at what point in the cross section of the channel the maximum current would occur.

One interesting feature of the current direction plots is that some boundary layer seems to exist at about 50 m. Above this layer, the current direction, and thus the velocity vector, generally rotates counter-clockwise whereas below this layer at a depth of 75 m the rotation is predominantly clockwise. However, at 50 m depth for all three stations the gross behaviour of the current direction consists of oscillations about some average direction (arithmetic average about 160 - 170^{o}, see Figs. 11 - 17). This behaviour can be more easily seen in the progressive velocity plots (Figures 25 - 31) in which the looping of current velocity vector will be counterclockwise or clockwise accordingly. The counterclockwise rotation of the current in the top layer is caused by a cross-channel slope current created due to the piling of water on the right side to the direction of the flow along the channel axis. The reversal of the rotation is due to the tilting of the interface layer between different water masses. This rotation of the current will be discussed further in the sections on Virtual Displacement.

Velocity Histograms

As indicated by the direction histograms (Figures 11 - 17), the current direction tends to cluster about the "up-" and the "down-channel" directions. The occurrence of the two clusters points to the tidal nature of the water current. A weak steady flow in the down-channel direction superimposed over the tidal flow of water is evident from the stronger peak in this direction. In the speed histograms, there are no well defined peaks although a relative maximum seems to occur at about 10-20 cm/sec for each meter. No attempt has been made to compute the time averages of the direction and of the speed since the average velocity formed from the combination of the two averages can be very misleading. A more meaningful average velocity can be obtained from the progressive velocity plot.

Current Components

Each of the components of the current velocity is enclosed by a lunar envelope as was the case for the current speed. In the period of a lunar day, generally two maxima and two minima occur in the major as well as in the minor component. Thus the currents are mainly

semi-diurnal in character. However, maxima occurring a lunar day apart are of approximately equal magnitude whereas neighbouring ones separated by about half a day are not. This of course is due to the presence of weaker diurnal components superimposed on the semi-diurnal ones. These components as well as others will be elucidated in the power spectra of the current components. Comparison between current components at different depths and stations will be made in a later section.

Virtual Displacement

For clarity the progressive vectors for each of the meters is plotted with the origin of the coordinate system displaced to the right of the diagram. To study these vectors, the coordinate origin should be translated without rotation to the starting point of these vectors.

The shapes of the current loops in the trajectories are highly irregular. Some are open loops while others are closed. Another loop may have started before the completion of the previous one. A clockwise rotation may become a counterclockwise one or vice versa. These complicated current trajectories are caused not only by the tides but also by the shoreline irregularities, bottom and sub-ice structures, atmospheric pressure difference and effects of wind stress on ice and open water elsewhere. It can be a considerable task even to sort out in detail some of the elementary features. Our discussion will be limited to the most salient and rudimentary ones.

The plots are made for the duration of immersion of the meters. A vector drawn from the start to the end of such a plot gives the "total displacement" from which an average velocity may be obtained for a fictitious parcel of water. If a meter stopped and re-started the above interpretation should be applied only to its initial period of proper operation. For such a meter, the progressive vector drawn for the whole period of immersion can nevertheless be useful since the direction of the total displacement vector may still be representative of that of the average current ,provided that its period of initial proper operation is sufficiently long.

The current loops of the trajectories for meters above 50 m are mainly counterclockwise (Figures 25 - 29 and 31) while those for the meter at 75 m are mostly clockwise (Figure 30). For the three meters at 50 m, the current loops are not as well developed as the others (Figures 25, 29 and 31). Generally there are two current loops (or parts of two loops) per lunar day and one of the two is usually more pronounced than the other one in accordance with the lunar inequalities. The sections

of the trajectory with large, well defined loops correspond to periods with large tidal oscillations whereas small and sometimes ill-defined loops result from (relatively) small fluctuating currents.

The peculiar feature of Station 3 (Figure 31) is that there appears to be a confusing number of current loops during a lunar day. A large-scale plot of the progressive vector from the beginning of its operation to May 24 2400 GMT shows that the complication arises from current loops embedded in other loops. (See inset in Figure 31). It is now easy to see the complicated trajectory for the period of large tidal oscillations (approximately May 24 to May 29) as being made up of such component parts.

All the trajectories lie within 190 - 215° from true north. This implies that the average water current superimposed on the sometimes large tidal oscillations flows approximately in the "down-channel" direction (230°) at the location of each meter. Arctic water is transported to the south through the channel effectively by these average currents the magnitude of which can be computed from selected lengths of records.

Power Spectra of the Current Components

The normalized power spectra of the current components are shown in Figures 32 - 38. The abscissa of these graphs is in frequency step of $\Delta f_o = 1.953 \times 10^{-3}$ CPH corresponding to the frequency resolution in the application of FFT to a record of 512 ($= 2^9$) hourly readings. The cut-off frequency is $256\Delta f_o = 1/2$ CPH which is the folding frequency for meters sampling at 60-minute interval. For meters sampling at 20-minute interval, 1/2 CPH corresponds only to a third of the folding frequency. However, there is no need to extend the power spectra since only noise seems to appear beyond this limit. The resolutions of these graphs are either in half-integral or in multiple steps of Δf_o depending on the length of the good continuous record available. The period in hours corresponding to the frequency scale is given in the upper part of these graphs.

From the power spectrum of either the major or the minor component of the current, it is possible to identify some of the component waves with tidal frequencies. The power density near f = 0 corresponds to the constant background flow of water through the location of the meter in the channel from the Arctic Ocean. This background current is the strongest at Station 1 and at 75 m of Station 2. The lunar fortnightly component of the current is not discernible, being either buried in the noise or swamped by the static component. The semi-diurnal components (periods about 12 hours) dominate over the components of other frequencies although the diurnal components (approximately 24 hours) are relatively strong. With the exception of the record from meter #234 at 75 m in Station 2, the other records are not long enough to resolve the different diurnal as well as the semi-diurnal components. For this meter, the semi-diurnal components M_2 and S_2 of periods 12.42 and 12.00 hours are discernible as are the diurnal components K_1 and O_1 of periods 23.93 and 25.82 hours (See Figure 37).

Perhaps one of the most interesting features of the power spectra is the presence of two other components of periods $\tau_1 \simeq 8.2$ and $\tau_2 \simeq 6.1$ hours, especially in the spectrum for the minor component of the current. These may be tidal oscillations but, if so, their amplitudes of oscillation are usually much smaller than the leading one at the diurnal frequencies. The present situation indicates that these amplitudes are approximately of the same order of magnitude (the root of the ratio of the power densities $\simeq 1$). Furthermore, if these oscillations are indeed tidal components at these frequencies, then the normalized power densities at either τ_1 or τ_2 for the major and minor components of the current should be about equal. However, the normalized power densities at these frequencies for the minor component of the current are larger than the corresponding quantities for the major component. Moreover, in the power spectrum for the tide at Lincoln Bay, obtained in the same fashion as the spectrum for either one of the velocity components, no significant power densities at these frequencies occur. All these seem to imply the presence of some cross-channel phenomenon of non-tidal origin. It is believed that τ_1 and τ_2 may be the periods of oscillation of internal waves at the interface separating different water masses.

Comparison of Current Velocities

In Figures 39 and 40, two sections of the current record in spring tide periods (May 10 - 14, May 24 - 28) are selected for comparison between different depths and between different stations. In the same figures the predicted water levels at Lincoln Bay and at Alert are also shown. Figures 41 and 42 show some of major and minor components in more detail.

From the time lag in the occurrence of high (or low) water levels at Lincoln Bay and at Alert, it is evident that the tide moves into Robeson Channel from Lincoln Sea. This time lag is approximately 1.2 hours. It is also easy to understand that the maximum current speed along the channel axis occurs before the high water. This lead time of the current is approximately 2 to 2.4 hours near Lincoln Bay.

The major components of the current appear to be in phase between different depths and between different stations. The amplitude of the current increases with depth down to 75 m. At 50 m the maximum down-channel current (maximum of major component) at Station 1 is slightly greater than that at the same depth for Station 2. The converse is generally true for the maximum of the up-channel current (minimum of major component). Thus a larger quantity of water flows down the channel at Station 1 than at Station 2 at this depth in a tidal cycle. The same statements as above, with "Station 3" replacing "Station 2", can be made from a comparison of meters at the same depth between Stations 1 and 3. No direct comparison is possible between Stations 2 and 3 because of the partial failure of one of the meters.

The transverse component of the current is more complicated than the major component in that the maximum-minimum oscillations exhibited by the latter are no longer clearcut. However, the cross-channel component

of the current is generally in phase at and above 50 m for all the stations. The amplitude of oscillation of the transverse current diminishes with increasing depth from 2.25 m to 50 m and then increases with a considerable phase shift at 75 m (Figure 42(a)). This component of the current at 50 and 75 m seems to exhibit almost twice as many oscillations as that at shallower depths. The double oscillations are very apparent during the weaker of any two consecutive semi-diurnal surges of the current (Figures 39(c), 40(a) and 42(b)). These multiple oscillations can be attributed to some interface layer passing through the meters at these depths thereby causing two reversals of the cross current for each oscillation of the interface.

In the top layer (less than 75 m), a down-channel current is generally accompanied by a transverse current towards Greenland. This cross current reverses its direction for an up-channel flow. In the stronger of the semi-diurnal tidal flows, this behaviour is well borne out but it becomes somewhat ill-defined in the weaker semi-diurnal oscillation. By the superposition of the transverse current over the longitudinal current together with a constant down-channel drift current in this layer, it is easy to see that the progressive vectors rotate counterclockwise. At 75 m, there is a phase shift in the transverse current relative to those in the top layer. At this depth, a longitudinal flow in one direction is accompanied by a transverse current flowing in one direction and then in the other. The phase shift is such that superposition of the longitudinal and transverse current results in a clockwise rotation of the current vector.

Figures 43 and 44(a) are composite plots of the progressive vectors for meters operating without malfunction in two common periods, May 4 - May 18 and May 24 - June 6, respectively. The opposite rotation of the current in the two layers can be followed in detail in Figure 44(b). From these trajectories, average currents can easily be computed for use in the calculation of the mass transport.

Average Current Profile

Figures 45 and 46 show the average current velocity profile obtained from the progressive vector plots (Figures 44 and 45). The average transverse current is directed towards Greenland and is very small (about 3 cm/sec except for Station 1). This transverse current remains fairly constant across the channel as well as with increasing depth. The down-channel component of the average current, however, increases with depth and also with the cross-channel distance from Greenland but it must vanish at the two shorelines. This average current at 50 m in Station 1 is almost as large as that at 75 m in Station 2. These average currents for the two locations are 10.6 and 10.4 cm/sec for the longitudinal component and 3.4 and 4.0 cm/sec for the transverse component. The "jet stream" in the channel, where the (average) current attains a maximum, is probably somewhere between Station 1 and Ellesmere Island and at a depth below 50 m.

An attempt can be made to construct an average current profile for the cross section of the channel for the purpose of computing the mass transport of water. This profile, however, can be representative only in a small region of the cross section in the vicinity of the three stations. The computed mass transport from such a current profile can be meaningless because of many still unknown crucial quantities. For instance, the location and the speed of the "jet stream" are not known. Moreover, the average current in the lower layer (about 500 m thick) was not measured in the work reported. An estimate of the mass transport will therefore be postponed until the presentation of the 1972 measurements which included observation at greater depths.

SUMMARY

The near-surface current observations in Robeson Channel have been given in different representations. The longitudinal and transverse components at different stations and at different depths have been compared. These components were also analyzed into frequency components for identification of the various tidal oscillations.

The current speed as well as each of the longitudinal and transverse components exhibited a lunar envelope with the maximum oscillation occurring approximately at full and new moon. The maximum down-channel current observed was about 75 cm/sec recorded at 75 m depth at Station 2. The longitudinal component of the current oscillates in phase between different stations and between different depths. The amplitude of oscillation increases with depth. During the down-channel flow in the semi-diurnal tidal oscillations, this longitudinal component exhibits a gradient across the channel towards Ellesmere Island. For the up-channel flow that follows, the gradient is reversed towards Greenland.

For the transverse component of the current, maximum speed of about 30 cm/sec was recorded at the 75 m depth. This current component is generally more complicated than the longitudinal component. Above and at 50 m, this component is in phase at different depths but a phase shift occurs at 75 m. This phase shift is responsible for the opposite rotation of the current in the two layers separated by an interface. There are two additional properties to note in the cross current. In contrast to the longitudinal component, its amplitude of oscillation decreases with depth above the interface (apparently near 50 m). Moreover, there seem to be twice as many oscillations in the cross component of the current for meters at 50 and 75 m as compared to the ones above these depths.

In the power spectra of the current velocity, most of the dominant tidal components can be readily identified. The lunar fortnightly as well as the several diurnal and semi-diurnal components are not well resolved because some records are too short. There were two components with periods $\tau_1 \simeq 8.2$ hours and $\tau_2 \simeq 6.1$ hours which were ruled out as being tidal in original because of their large power densities (compared to that of the leading diurnal component) and because the power density for the minor component was larger than that for the major component.

More importantly, to the same degree of resolution as in these power spectra, the spectrum of the tide at Lincoln Bay showed no significant oscillations at these frequencies.

The location in the cross section of the channel where the maximum of the current would occur is not known. The near-surface measurements are also insufficient to determine the depth at which the maximum current flows. The average current velocity indicates that there is a constant, small cross current (about 3 cm/sec) towards Greenland. The average longitudinal current is down-channel and it increases with depth and with distance towards Ellesmere Island. At Station 2, this average current increases almost linearly from 2.5 to 10 cm/sec from depth 2.25 to 75 m. Across the channel this increase at the 50 m depth is from 4 to 10 cm/sec from Station 3 to Station 1. No mass transport estimate was attempted because of the small region spanned by the array of meters.

A simple model of the channel consisting of a sloping sea surface together with a density interface tilted in the opposite direction can produce the observed near-surface current pattern and it will be proposed in a follow-up report. It will be shown that the longitudinal and transverse current profiles follow quite naturally from this model. The multiple reversal of the transverse current near 50 m can be the result of the interface passing through these depths thereby causing the cross current to change its direction twice for each complete oscillation of the surface. The two persistent non-tidal components in the power spectra are also seen as due to the free internal oscillations of the density interfaces.

REFERENCES

1. Keys, John E., Moira Dunbar, D.J. Finlayson and J.W. Moffat, Radar Measurement of Ice Drift in Robeson Channel, 1972. DREO Tech. Note 74-21, 1974.

2. Sadler, H.E., Movement of Water and Ice Through Robeson Channel, Doctoral Thesis submitted to Dalhousie University, 1974.

3. Finlayson, D.J., Techniques for deploying surface and submerged recording instruments in the waters of the Canadian Archipelago. DREO Tech. Note 72-29, 1972.

4. See for instance Gerhard Newmann and Willard J. Pierson, Jr., Principles of Physical Oceanography. Prentice-Hall Inc., Englewood Cliffs, N.J., 1966.

5. Blackman, R.B. and J.W. Tukey, The Measurement of Power Spectra from the Point of View of Communications Engineering. Dover Publications, Inc., New York, N.Y., 1958.

6. Jenkins, Gwilyn M. and Donald G. Watts, Spectral Analysis and its Applications. Holden-Day, Inc., San Francisco, Calif. 1968, Chapters 5 and 6, pp. 140-257.

7. Cooley, J.W., P.A.W. Lewis and P.D. Welsh, Applications of the Fast Fourier Transform to Computation of Fourier Integrals, Fourier Series and Convolution Integrals. IEEE Trans. Audio and Electroacoustics, Vol AU-15, No. 2, June 1967, pp 79-84.

ACKNOWLEDGEMENT

The author wishes to thank Mr. G.C. Dohler and his group in Tides and Water Levels of Environment Canada for analyzing the Lincoln Bay water level data and for providing tide predictions at Alert and Lincoln Bay.

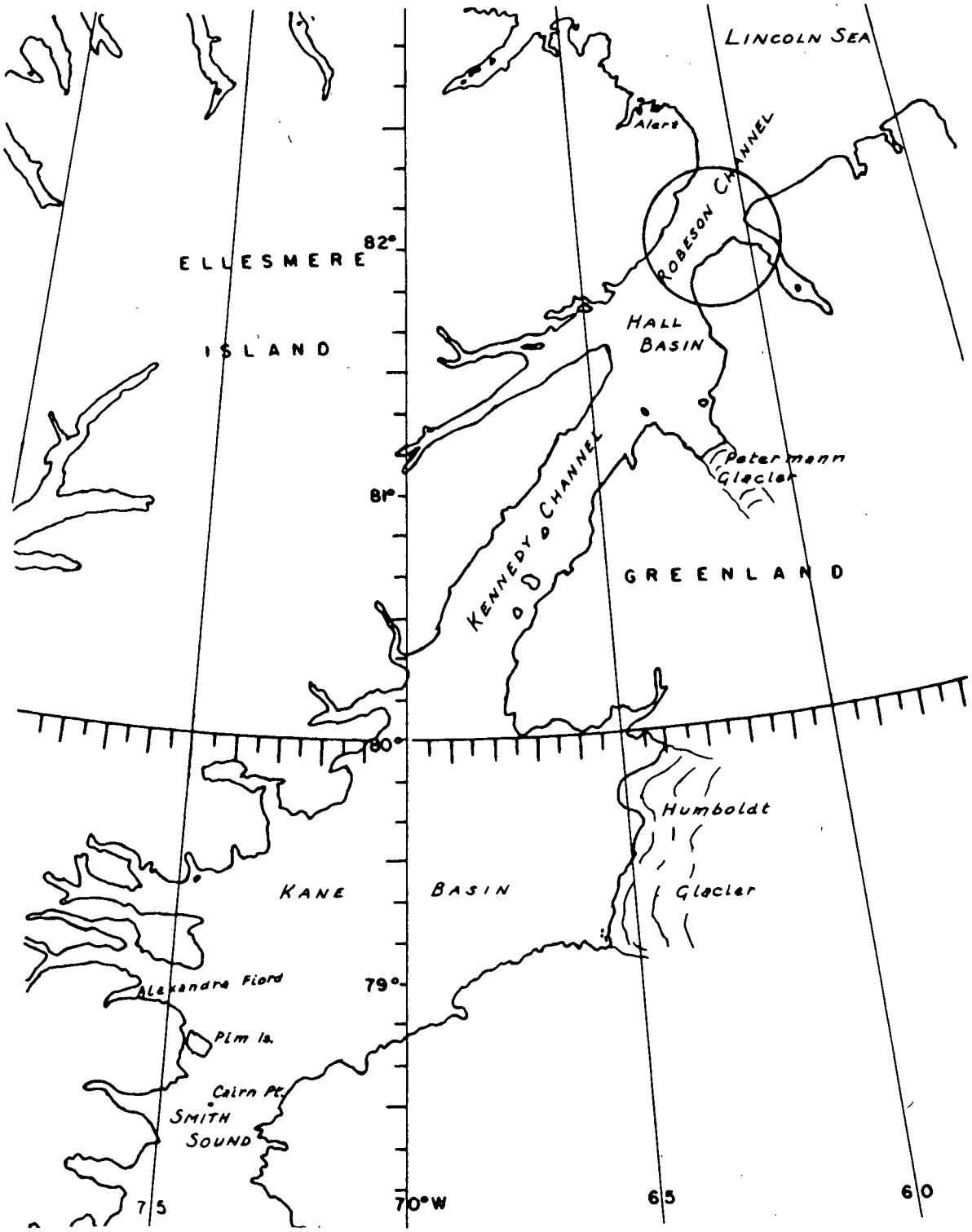

Fig. 1 Map showing northern section of Nares Strait. Encircled area of Robeson Channel indicates area of 1971 spring operation.

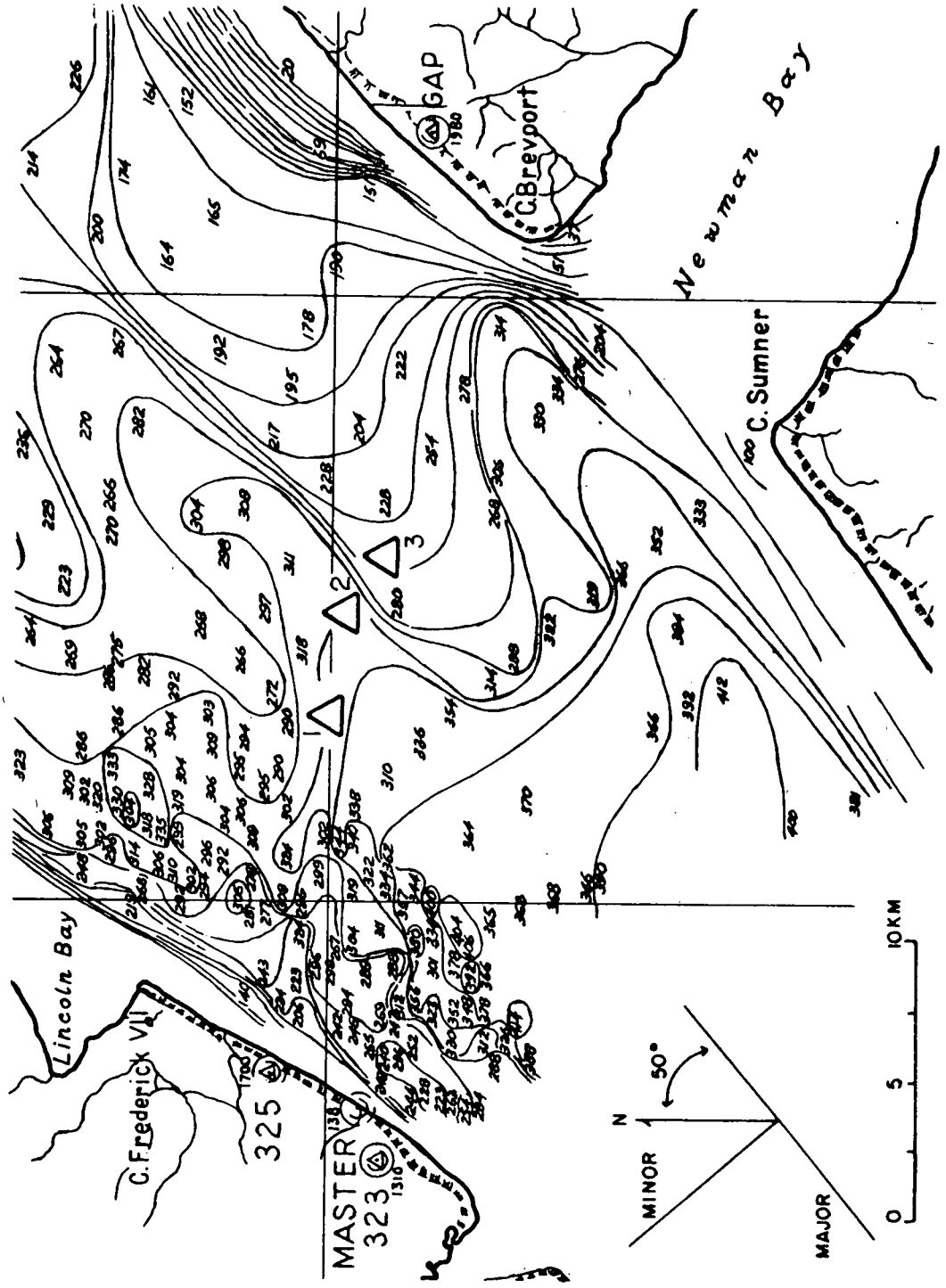

Fig. 2 *A more detailed map of section of Robeson Channel. Numbered triangles indicate approximate locations of the three stations and the coordinate system used in report is illustrated at lower left. (Depth in fathoms and height in feet).*

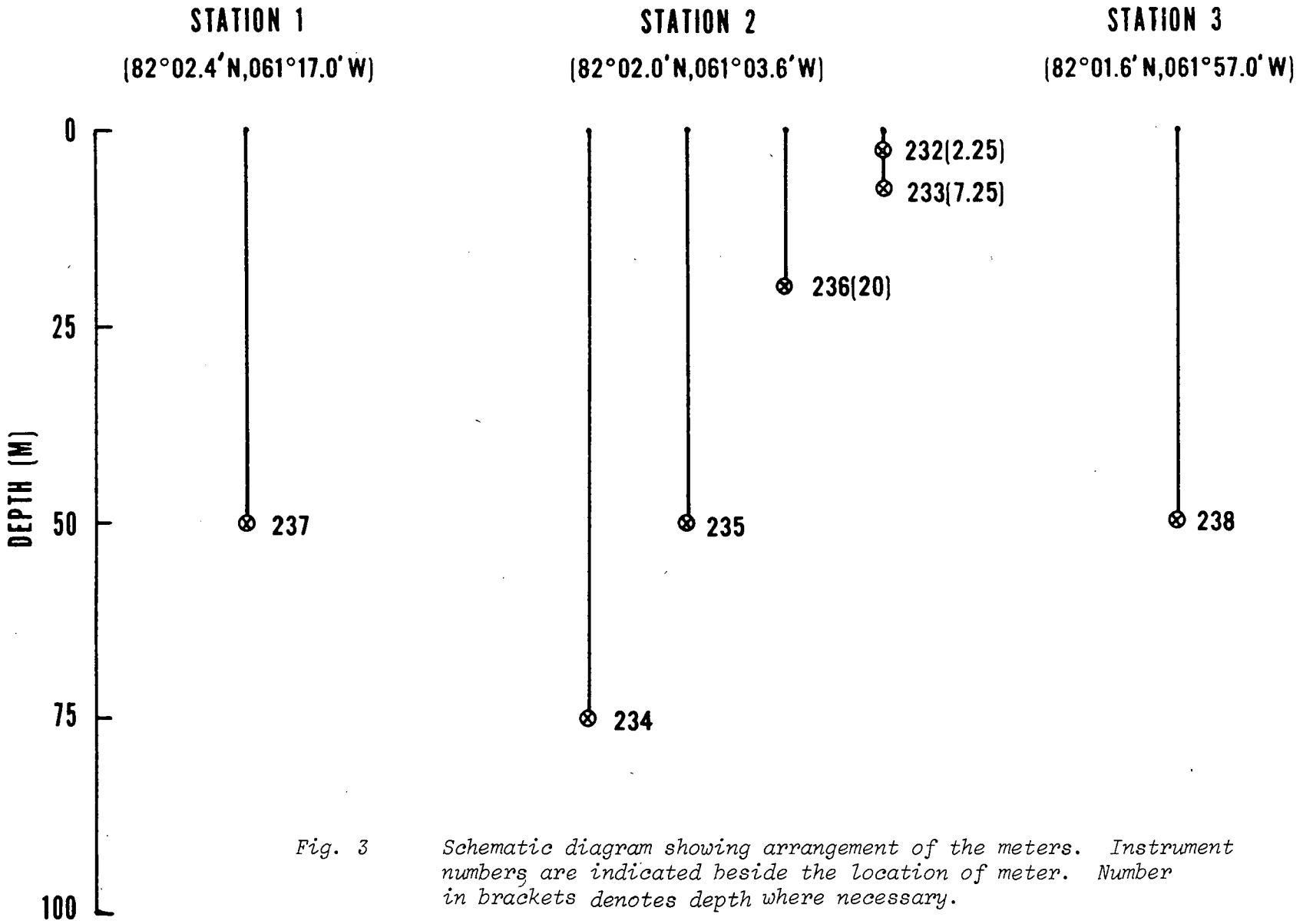

Fig. 3 *Schematic diagram showing arrangement of the meters. Instrument numbers are indicated beside the location of meter. Number in brackets denotes depth where necessary.*

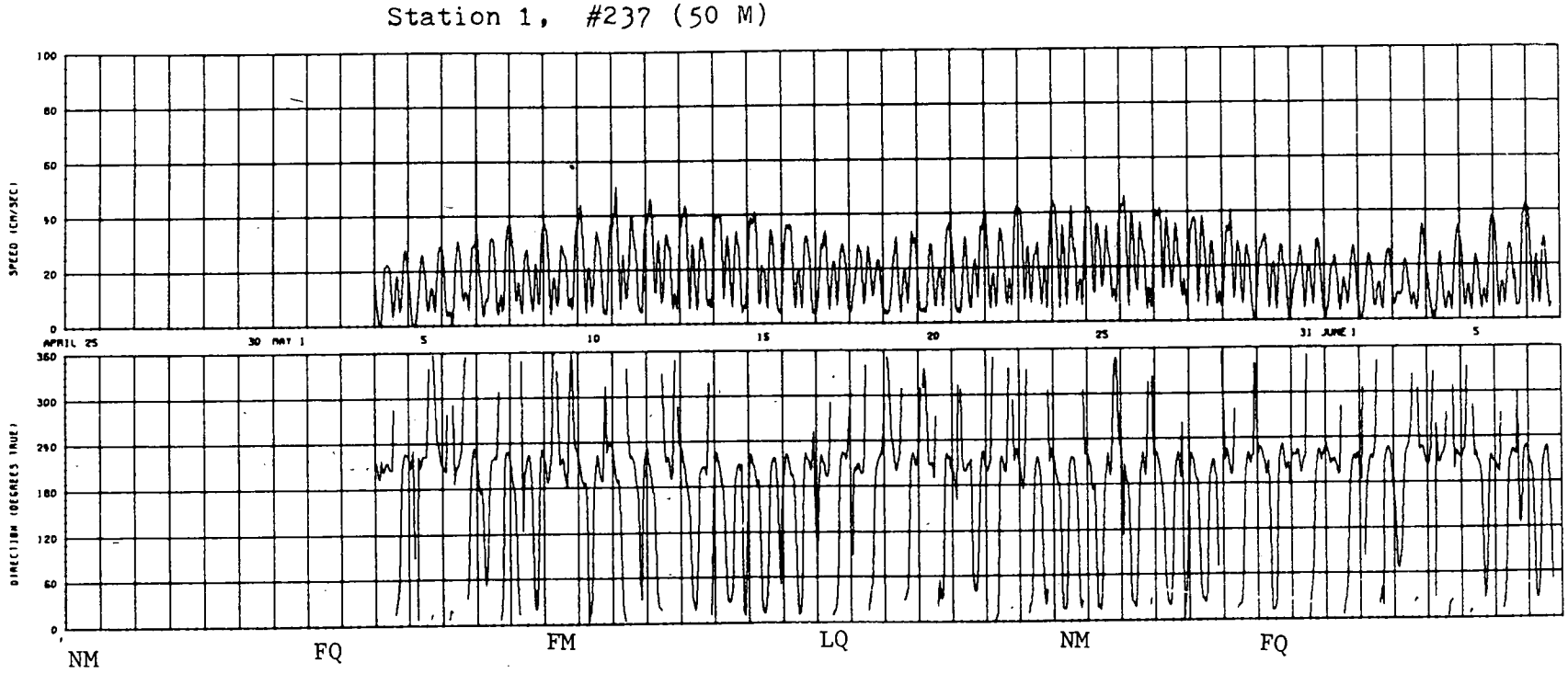

Fig. 4 *Speed and direction of current. The time of occurence of the phases of moon are indicated approximately with NM, FQ, FM and LQ denoting new moon, first quarter, full moon and last quarter.*

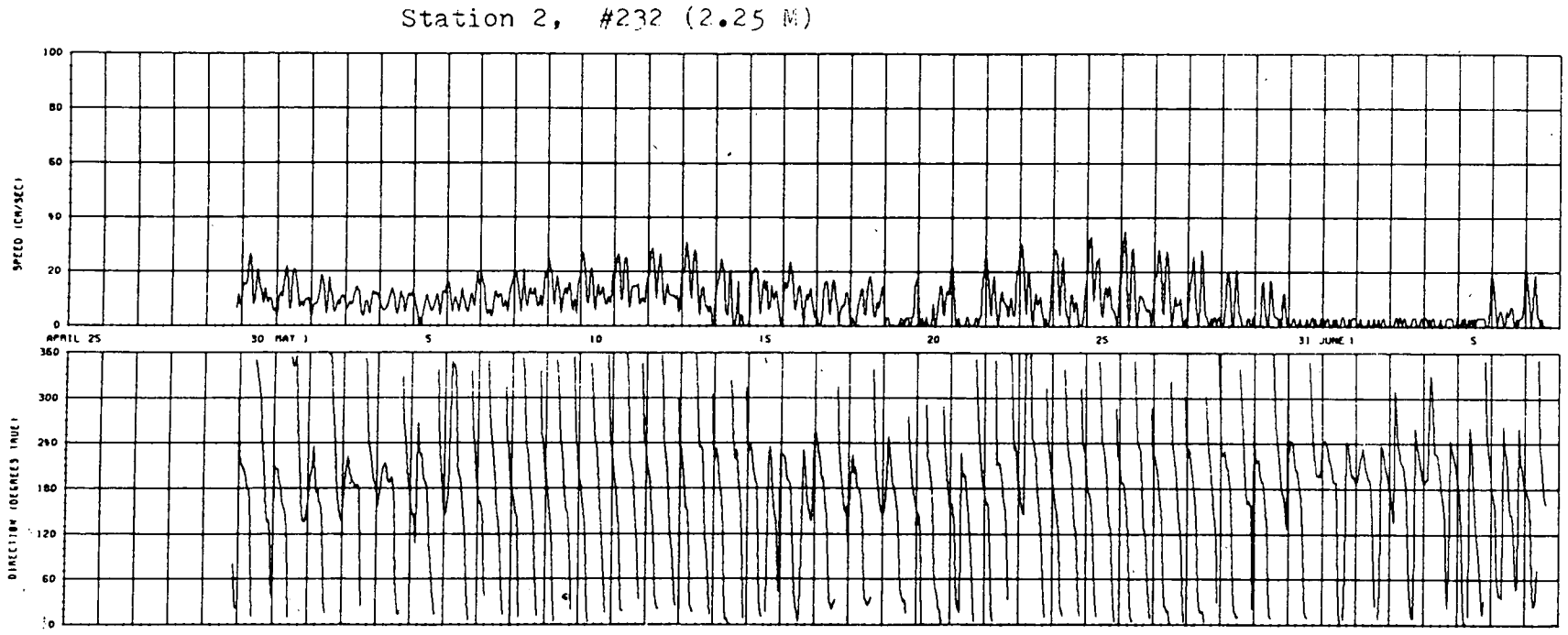

Fig. 5 Speed and direction of current.

UNCLASSIFIED

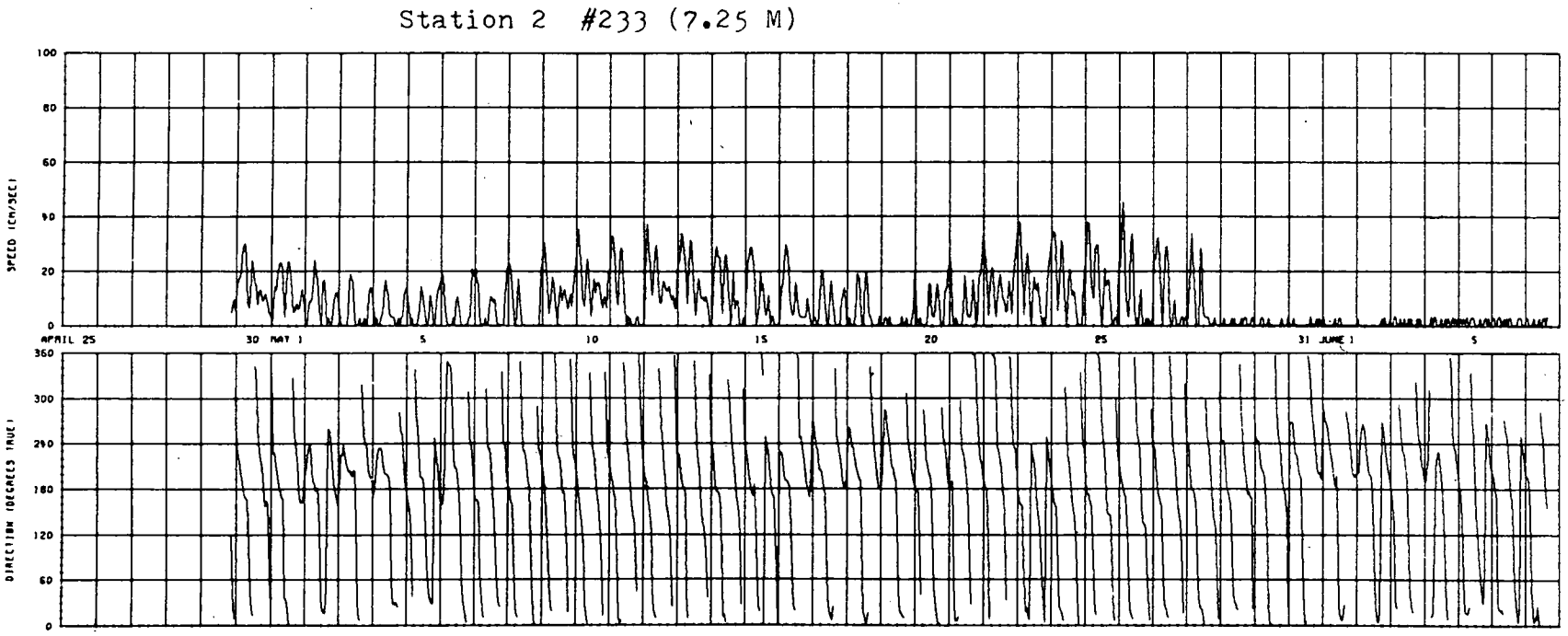
Station 2 #233 (7.25 M)
SPEED (CM/SEC)
100
80
60
40
20
0
APRIL 25
30
MAY 1
5
10
15
20
25
31
JUNE 1
5
DIRECTION (DEGREES TRUE)
360
300
240
180
120
60
0

Fig. 6 *As Fig. 5.*

Station 2, #236 (20 M)

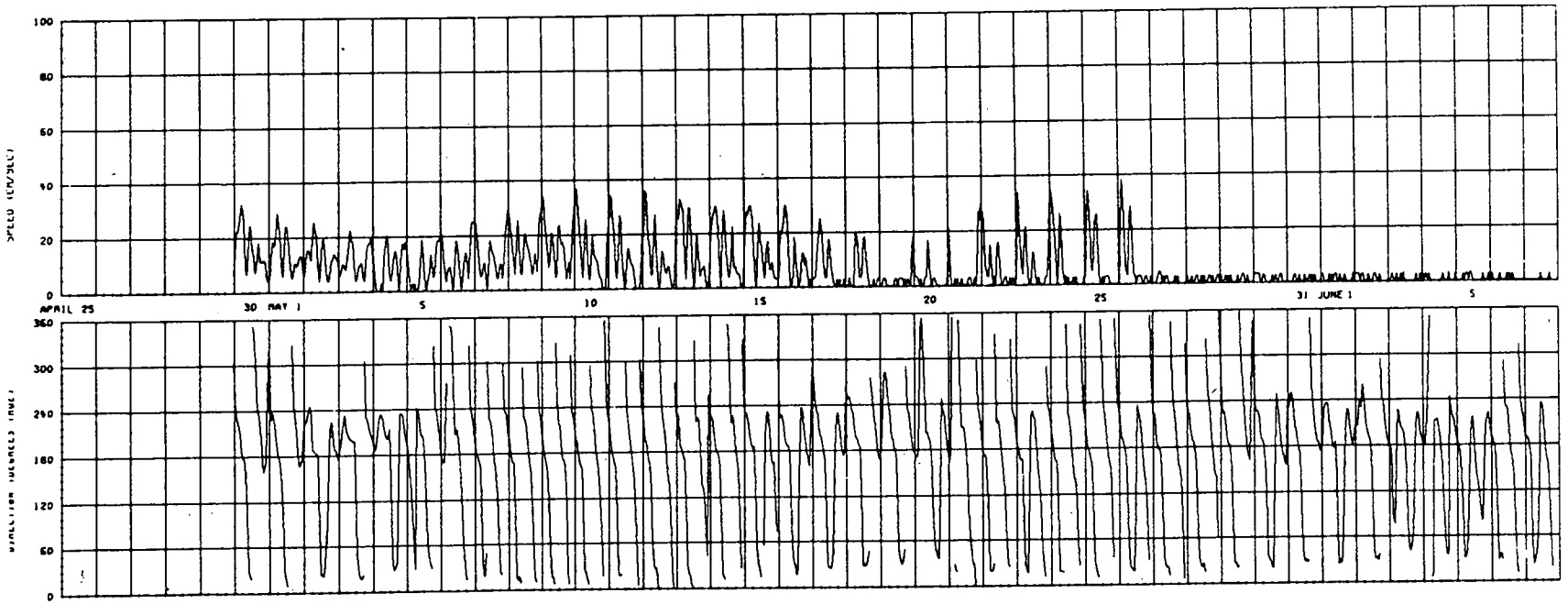

Fig. 7 As *Fig. 5.*

Station 2, #235 (50 M)

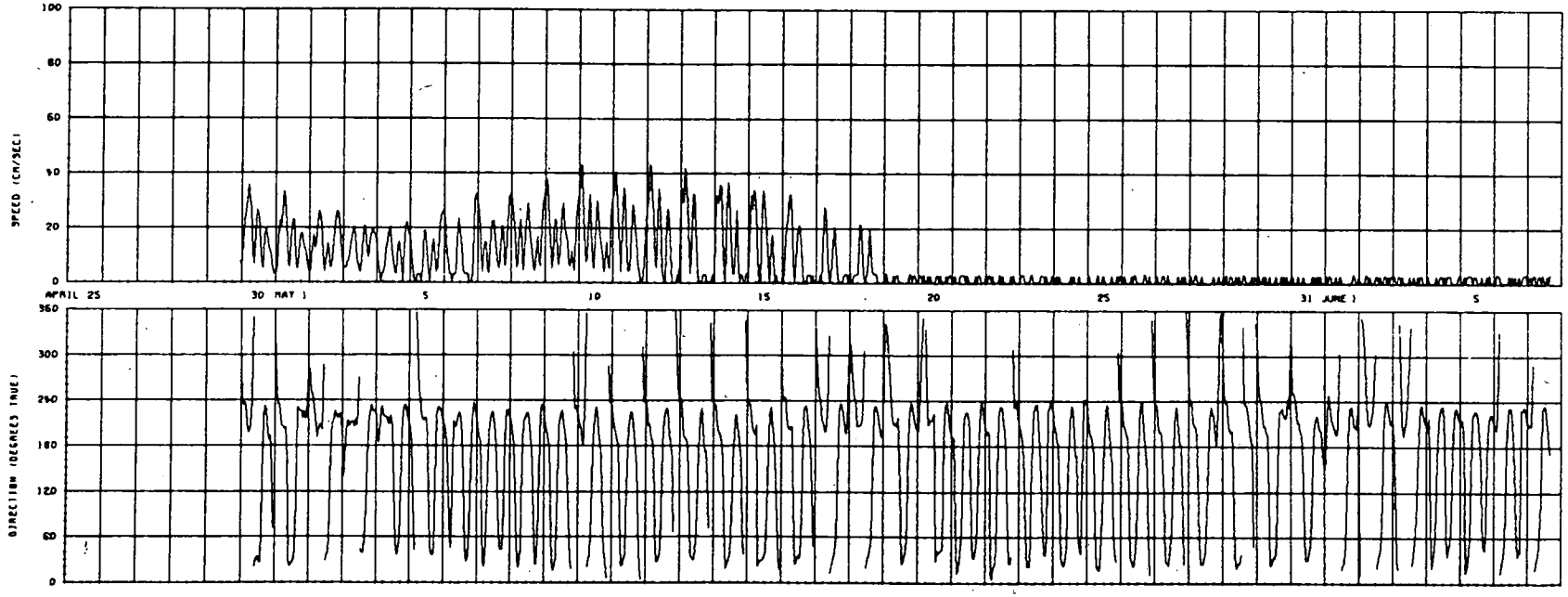

Fig. 8. *As Fig. 5.*

UNCLASSIFIED

Station 2, #234 (75 M)

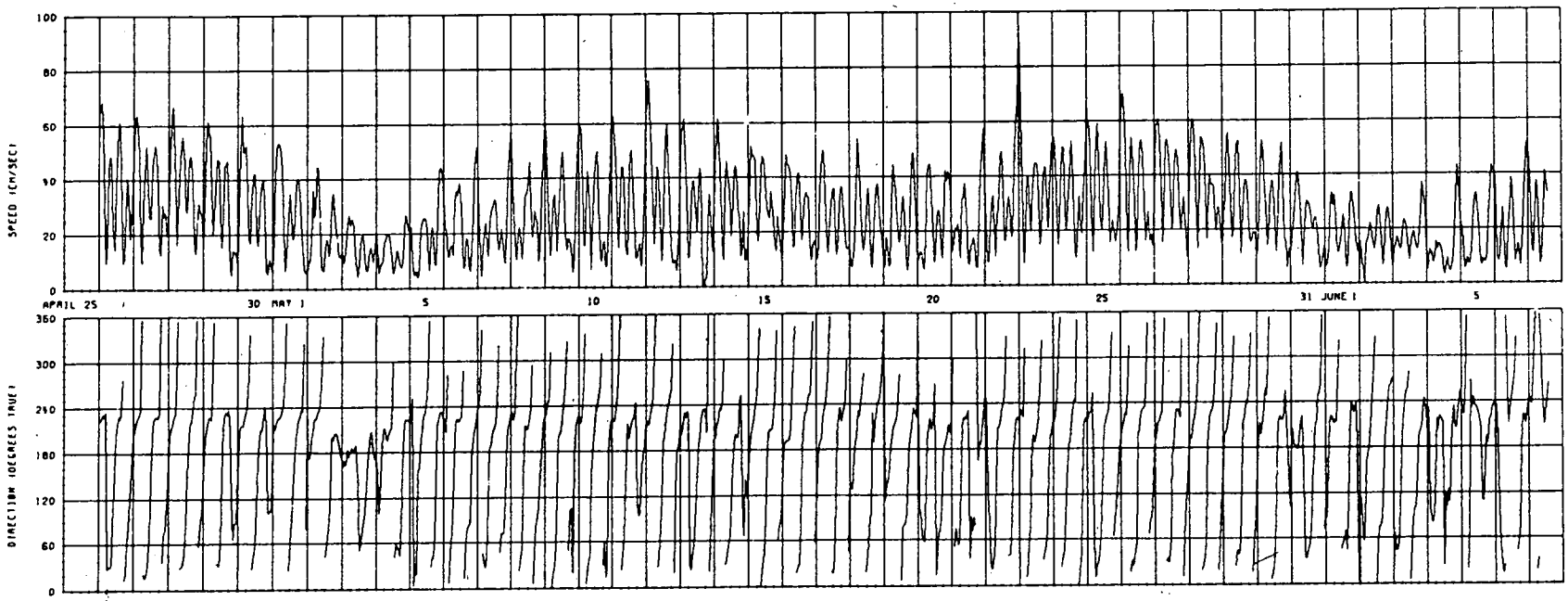

Fig. 9. *As Fig. 5.*

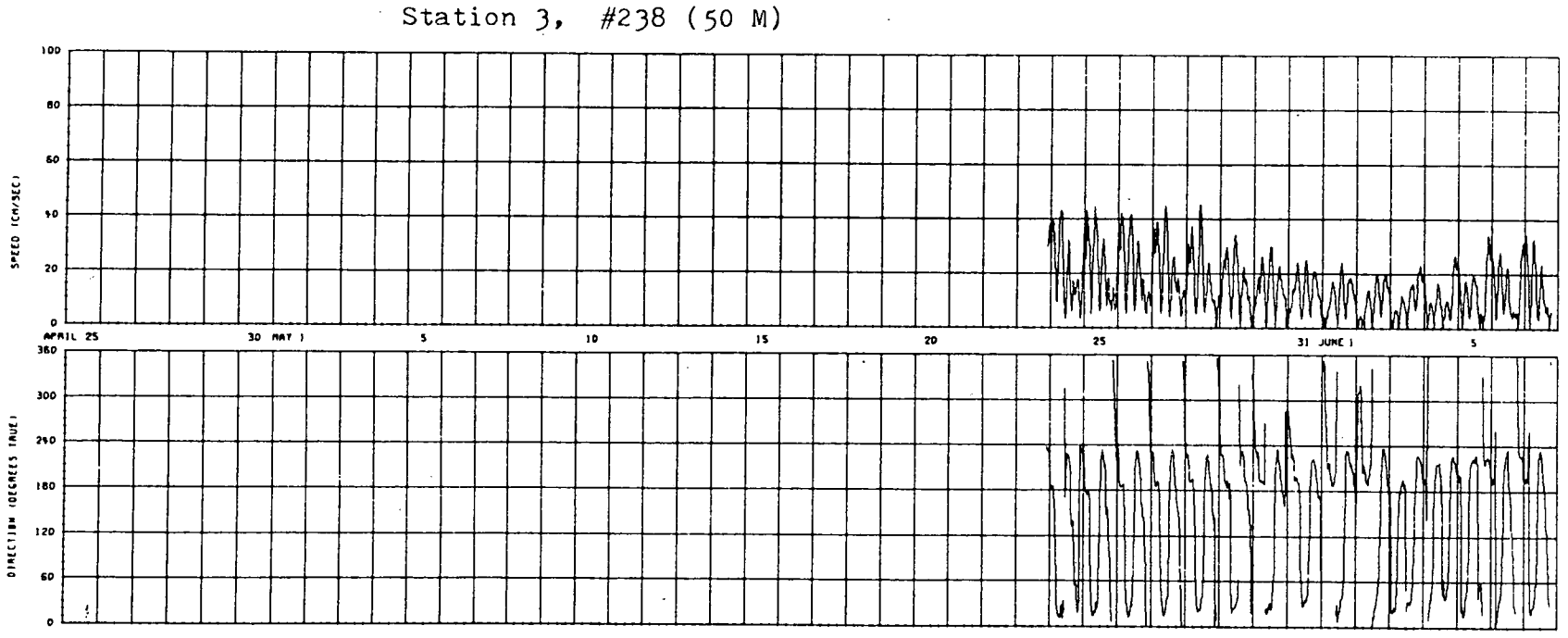

Fig. 10 *As Fig. 5.*

Station 1, #237 (50 M)

DIRECTION HISTOGRAM

NO. OBS	DIRECTION (DEG TRUE)	
18	0- 9	**********
42	10- 19	**************************
50	20- 29	*********************************
25	30- 39	*****************
15	40- 49	**********
10	50- 59	******
12	60- 69	********
7	70- 79	****
10	80- 89	******
7	90- 99	****
6	100-109	****
12	110-119	********
8	120-129	*****
12	130-139	********
8	140-149	*****
5	150-159	***
11	160-169	*******
19	170-179	**********
47	180-189	******************************
64	190-199	**
107	200-209	**
125	210-219	**
97	220-229	**
22	230-239	**************
7	240-249	****
6	250-259	****
8	260-269	*****
8	270-279	*****
8	280-289	*****
5	290-299	***
10	300-309	******
8	310-319	*****
7	320-329	****
11	330-339	*******
6	340-349	****
11	350-359	*******
834		

SPEED HISTOGRAM

NO. OBS	SPEED CM/SEC	
27	0- 3	**********
41	4	*********************
161	5- 9	**
127	10- 14	***
91	15- 19	**
104	20- 24	**
118	25- 29	**
72	30- 34	**********************************
53	35- 39	**************************
37	40- 44	*******************
2	45- 49	*
1	50- 54	
834		

Fig. 11 Speed and direction histograms. The first line in the speed histogram represents the threshold speed of the meter.

Station 2, #232 (2.25 M)

DIRECTION HISTOGRAM

NO. OBS	DIRECTION (DEG TRUE)	
32	0- 9	**********
41	10- 19	**********
35	20- 29	**********
30	30- 39	**********
19	40- 49	**********
9	50- 59	**********
13	60- 69	**********
11	70- 79	**********
11	80- 89	**********
7	90- 99	**********
16	100-109	**********
12	110-119	**********
15	120-129	**********
25	130-139	**********
45	140-149	**********
39	150-159	**********
35	160-169	**********
44	170-179	**********
59	180-189	**********
62	190-199	**********
47	200-209	**********
48	210-219	**********
54	220-229	**********
50	230-239	**********
37	240-249	**********
7	250-259	**********
14	260-269	**********
9	270-279	**********
8	280-289	**********
11	290-299	**********
10	300-309	**********
10	310-319	**********
8	320-329	**********
9	330-339	**********
20	340-349	**********
29	350-359	**********
931		

SPEED HISTOGRAM

NO. OBS	SPEED CM/SEC	
299	0- 3	**********
58	4	**********
201	5- 9	**********
185	10- 14	**********
95	15- 19	**********
57	20- 24	**********
29	25- 29	**********
6	30- 34	**********
1	35- 39	
931		

Fig. 12 As Fig. 11.

Station 2, # 233 (7.25 M)

DIRECTION HISTOGRAM

NO. OBS	DIRECTION (DEG TRUE)	
50	0- 9	**********
53	10- 19	**********
41	20- 29	********
26	30- 30	*****
10	40- 49	**
10	50- 59	**
5	60- 69	*
12	70- 79	**
6	80- 89	*
7	90- 99	*
12	100-109	**
10	110-119	**
15	120-129	***
14	130-139	***
17	140-149	***
26	150-159	*****
39	160-169	********
52	170-179	**********
50	180-189	**********
69	190-199	**************
57	200-209	**********
39	210-219	********
55	220-229	**********
59	230-239	**********
40	240-249	********
28	250-259	*****
18	260-269	***
12	270-279	**
16	280-289	***
7	290-299	*
8	300-309	*
12	310-319	**
7	320-329	*
15	330-339	***
10	340-349	**
25	350-359	*****

932

SPEED HISTOGRAM

NO. OBS	SPEED CM/SEC	
462	0- 3	**********
54	4	*
98	5- 9	**
111	10- 14	**
75	15- 19	**
60	20- 24	*
38	25- 29	*
26	30- 34	*
7	35- 39	*
0	40- 44	
1	45- 49	

932

Fig. 13 As Fig. 11.

Station 2, #236 (20 M)

DIRECTION HISTOGRAM

NO. OBS	DIRECTION (DEG TRUE)	
17	0- 9	******************
47	10- 19	**
61	20- 29	**
39	30- 39	***
17	40- 49	******************
14	50- 59	***************
10	60- 69	**********
10	70- 79	**********
5	80- 89	*****
10	90- 99	**********
15	100-109	**************
11	110-119	**********
12	120-129	************
14	130-139	***************
18	140-149	******************
28	150-159	*****************************
43	160-169	***
66	170-179	**
75	180-189	**
56	190-199	***
58	200-209	**
53	210-219	***
76	220-229	**
63	230-239	***
17	240-249	******************
12	250-259	************
8	260-269	********
7	270-279	*******
7	280-289	*******
11	290-299	**********
8	300-309	********
6	310-319	******
9	320-329	*********
3	330-339	***
12	340-349	************
14	350-359	**************

932

SPEED HISTOGRAM

NO. OBS	SPEED CM/SEC	
481	0- 3	**
52	4	*********
112	5- 9	********************
95	10- 14	*****************
71	15- 19	*************
55	20- 24	*********
45	25- 29	*******
17	30- 34	***
4	35- 39	*

932

Fig. 14 As Fig. 11.

Station 2, #235 (50 M)

DIRECTION HISTOGRAM

NO. OBS	DIRECTION (DEG TRUE)	
5	0- 9	****
22	10- 19	******************
67	20- 29	**********
61	30- 39	**********
39	40- 49	**********
20	50- 59	**********
12	60- 69	**********
11	70- 79	**********
11	80- 89	**********
12	90- 99	**********
6	100-109	*****
11	110-119	**********
14	120-129	**********
10	130-139	**********
14	140-149	**********
11	150-159	**********
19	160-169	**********
16	170-179	**********
34	180-189	**********
70	190-199	**********
94	200-209	**********
87	210-219	**********
98	220-229	**********
92	230-239	**********
24	240-249	**********
7	250-259	******
5	260-269	*****
3	270-279	**
7	280-289	******
4	290-299	***
9	300-309	*******
5	310-319	****
6	320-329	*****
5	330-339	****
10	340-349	********
8	350-359	*******

930

SPEED HISTOGRAM

NO. OBS	SPEED CM/SEC	
558	0- 3	**********
49	4	*******
70	5- 9	**********
61	10- 14	**********
58	15- 19	**********
49	20- 24	*******
39	25- 29	******
34	30- 34	*****
6	35- 39	*
6	40- 44	*

930

Fig. 15 As Fig. 11.

Station 2, #234 (75 M)

DIRECTION HISTOGRAM

NO. OBS	DIRECTION (DEG TRUE)	
13	0- 9	**********
27	10- 19	**********
32	20- 29	**********
34	30- 39	**********
35	40- 49	**********
33	50- 59	**********
22	60- 69	**********
28	70- 79	**********
31	80- 89	**********
14	90- 99	**********
26	100-109	**********
15	110-119	**********
11	120-129	********
14	130-139	**********
18	140-149	**********
17	150-159	**********
23	160-169	**********
18	170-179	**********
42	180-189	**********
46	190-199	**********
60	200-209	**********
94	210-219	**********
106	220-229	**********
86	230-239	**********
37	240-249	**********
30	250-259	**********
18	260-269	**********
11	270-279	********
11	280-289	********
10	290-299	********
5	300-309	****
7	310-319	*****
12	320-329	*********
7	330-339	*****
5	340-349	****
24	350-359	**********
1022		

SPEED HISTOGRAM

NO. OBS	SPEED CM/SEC	
6	0- 3	***
5	4-	***
114	5- 9	**********
145	10- 14	**********
127	15- 19	**********
116	20- 24	**********
110	25- 29	**********
91	30- 34	**********
73	35- 39	**********
71	40- 44	**********
62	45- 49	**********
49	50- 54	**********
27	55- 59	**********
14	60- 64	********
8	65- 69	****
1	70- 74	*
2	75- 79	*
0	80- 84	
0	85- 89	
1	90- 94	*
1022		

Fig. 16 As Fig. 11.

Station 3 , #238 (50 M)

DIRECTION HISTOGRAM

NO. OBS	DIRECTION (DEG TRUE)	
14	0- 9	*********
57	10- 19	************************************
84	20- 29	**
72	30- 39	**
26	40- 49	*****************
37	50- 59	************************
15	60- 69	**********
8	70- 79	*****
10	80- 89	*******
13	90- 99	*********
7	100-109	*****
8	110-119	*****
10	120-129	*******
17	130-139	**********
27	140-149	******************
16	150-159	**********
18	160-169	************
37	170-179	************************
84	180-189	**
112	190-199	**
50	200-209	**********************************
81	210-219	***
119	220-229	**
54	230-239	************************************
9	240-249	******
9	250-259	******
9	260-269	******
6	270-279	****
11	280-289	*******
2	290-299	*
3	300-309	**
11	310-319	*******
6	320-329	****
12	330-339	********
9	340-349	******
12	350-359	********

1074

SPEED HISTOGRAM

NO. OBS	SPEED CM/SEC	
76	0- 3	************************
54	4	********************
154	5- 9	**
71	10- 14	**
156	15- 19	**
119	20- 24	**
90	25- 29	******************************
60	30- 34	**********************
33	35- 39	************
24	40- 44	********
3	45- 49	*

1074

Fig. 17 As Fig 11.

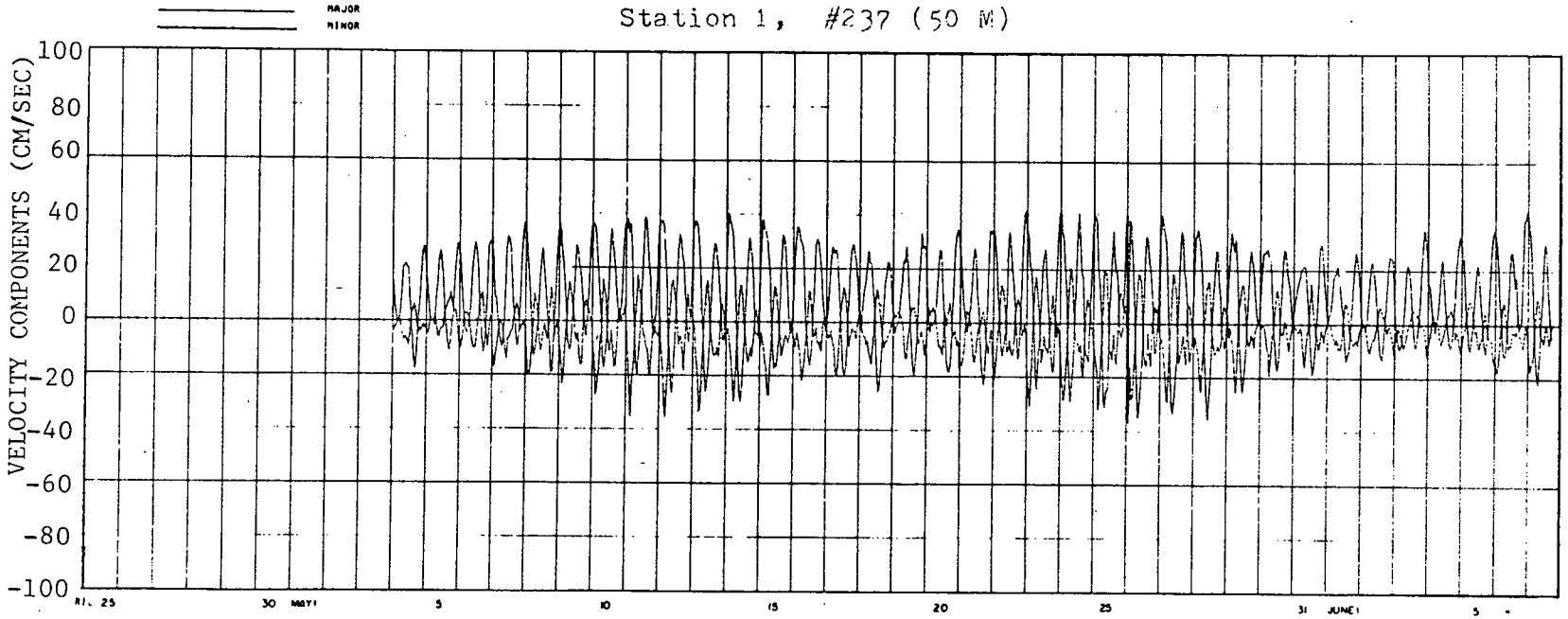

Fig. 18 Major and minor components of the current.

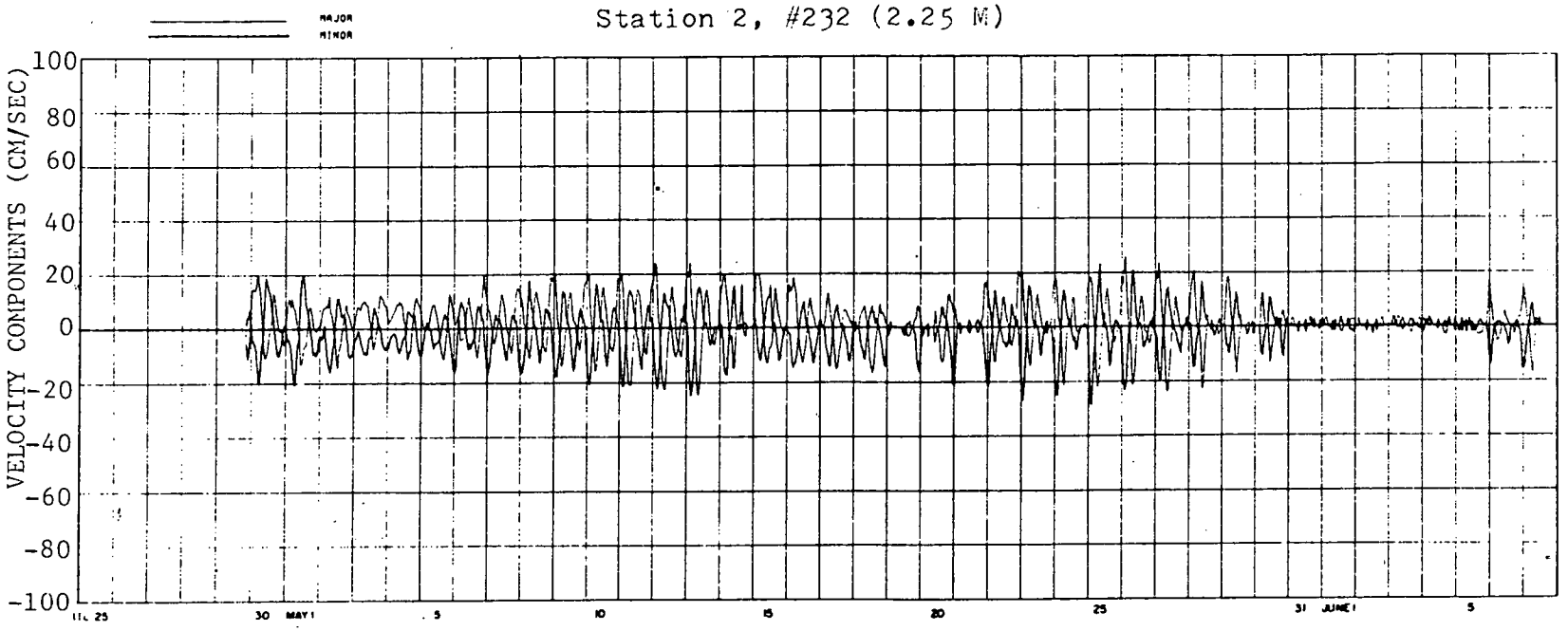

Fig. 19 *As Fig. 18.*

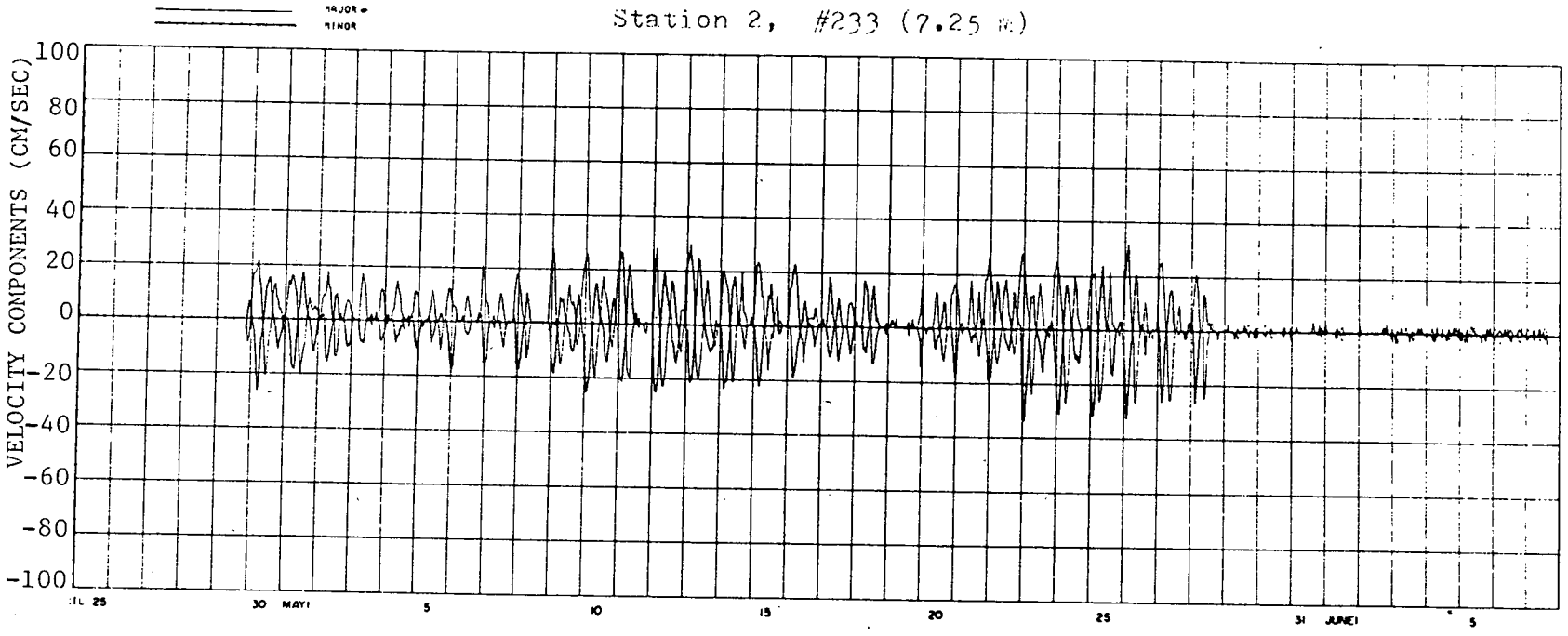

Fig. 20 *As Fig. 18*

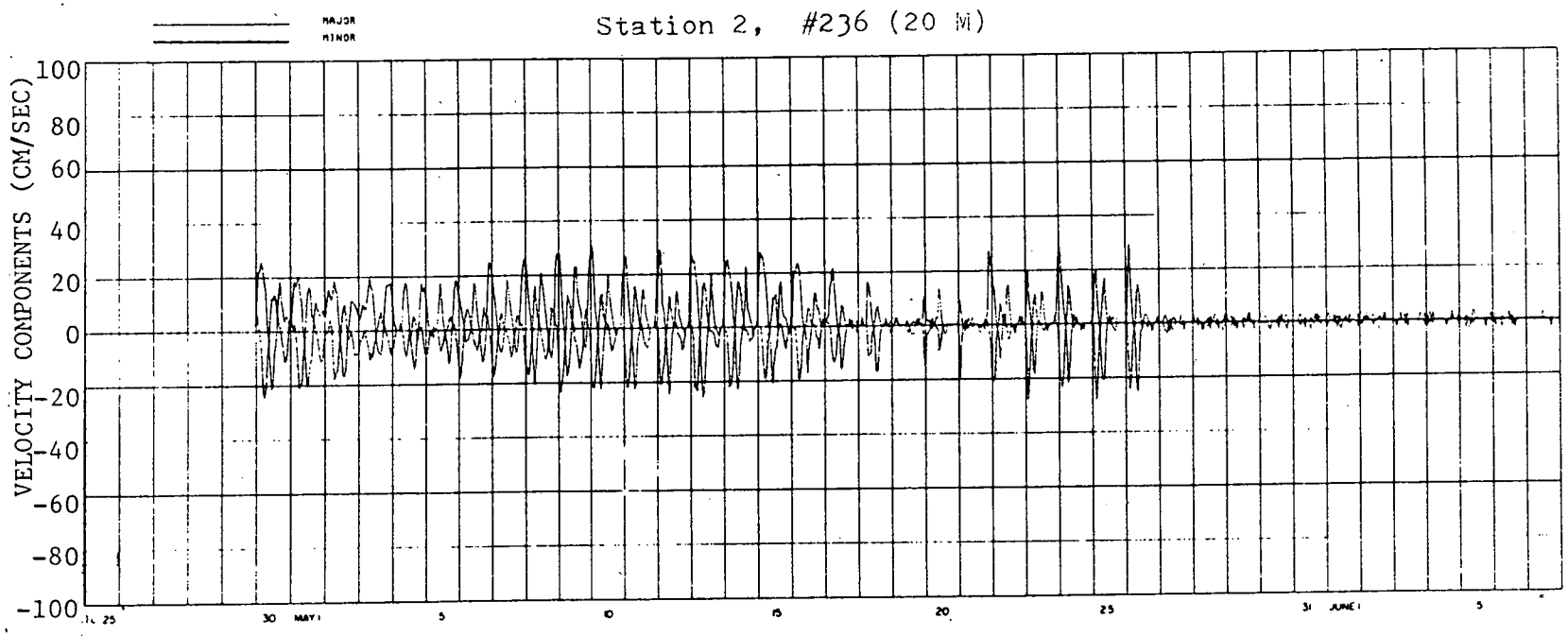

Fig. 21 As Fig. 18

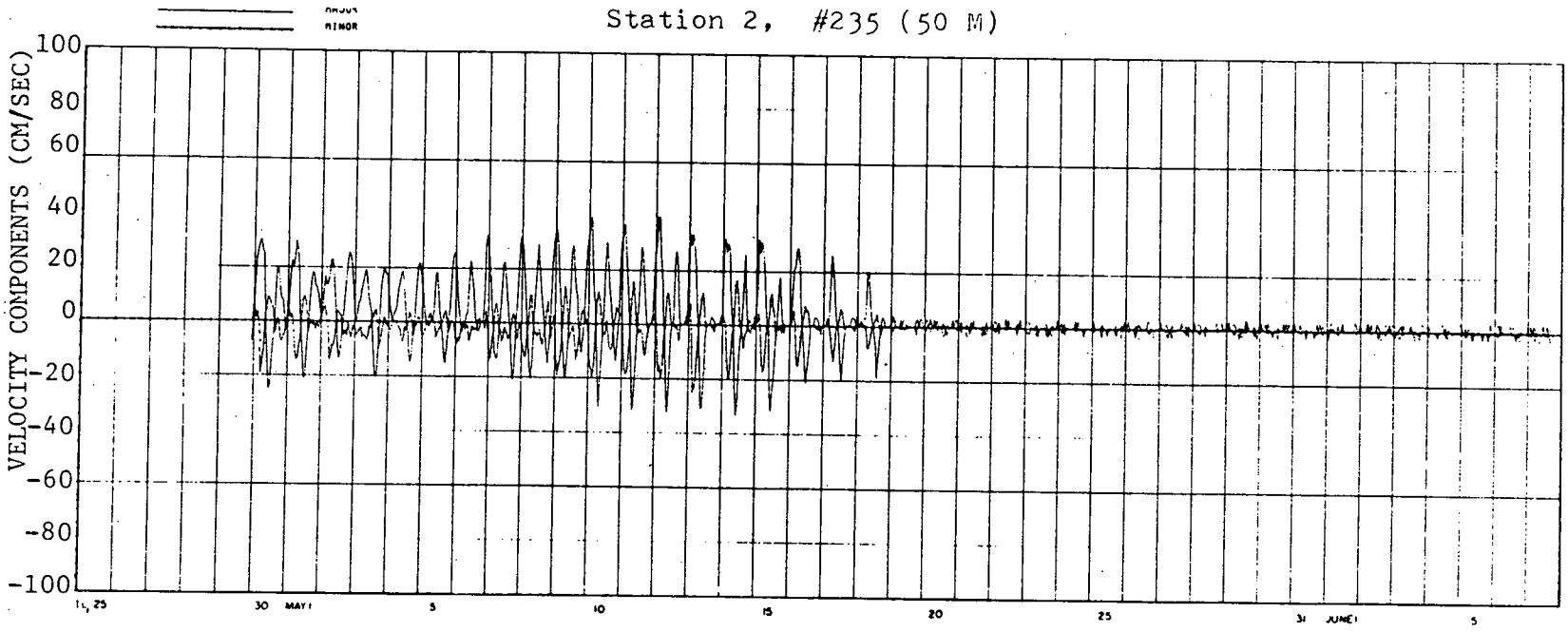

Fig. 22 *As Fig. 18*

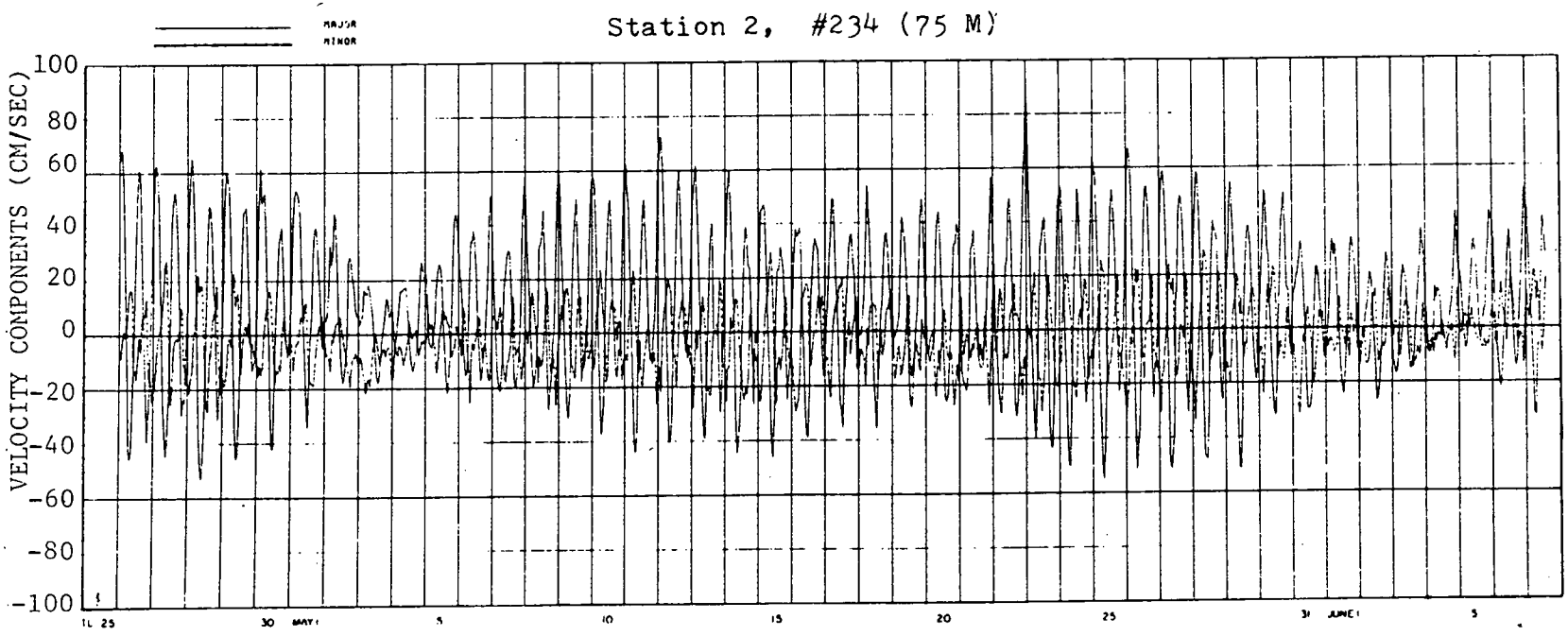

Fig. 23 As Fig. 18

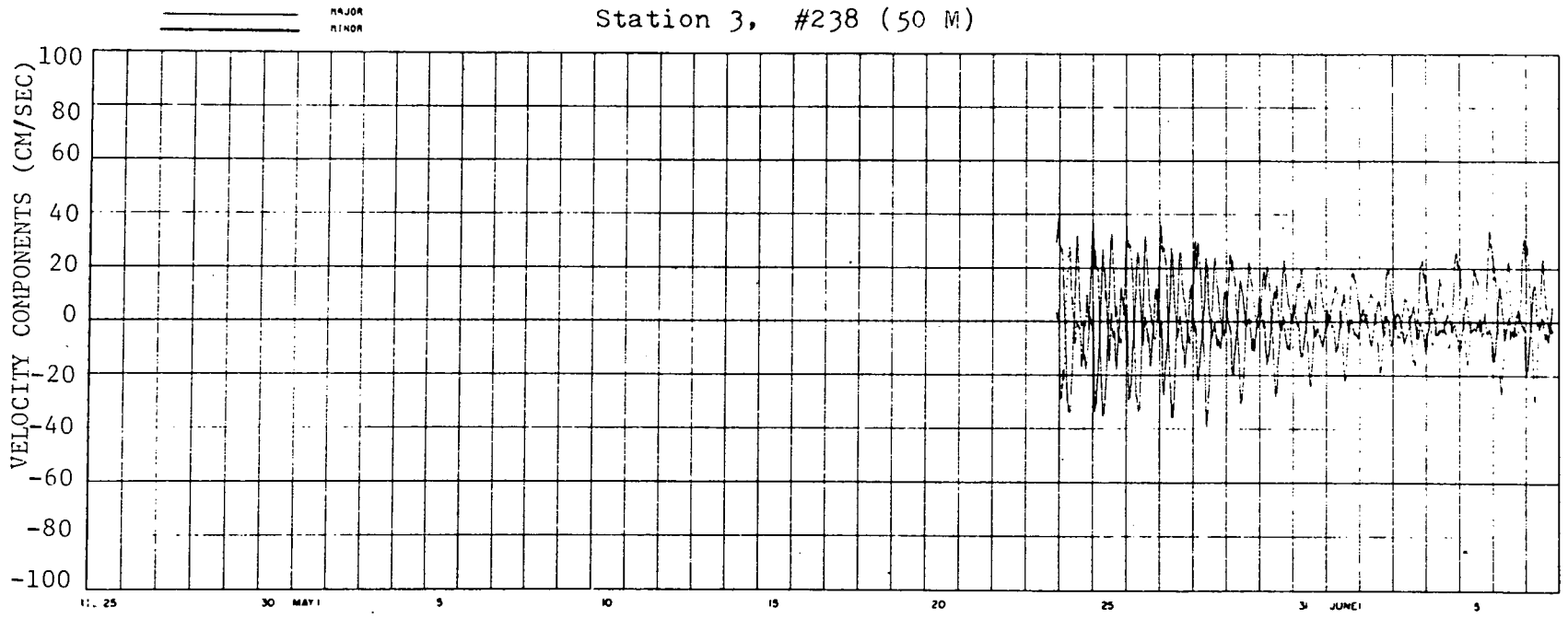

Fig. 24 As Fig. 18

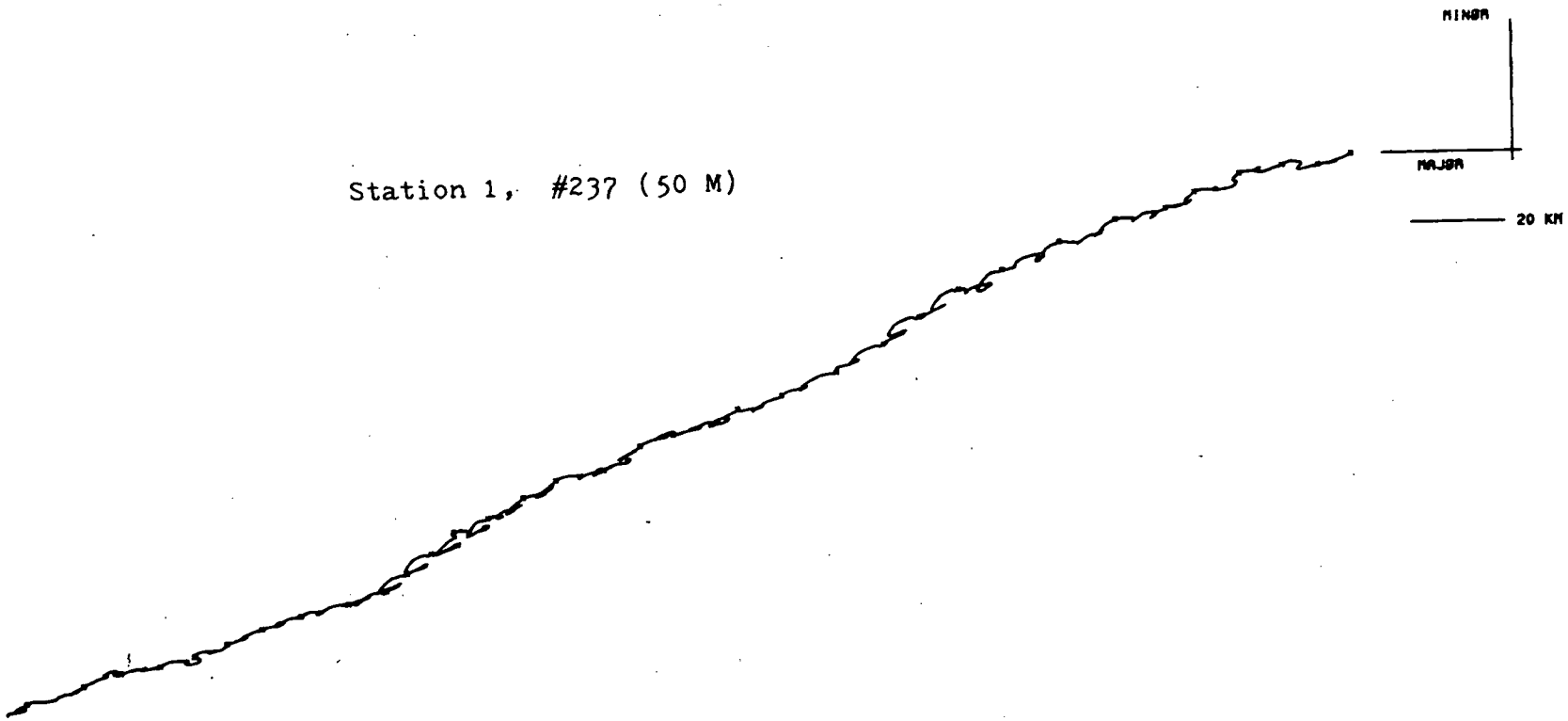

Fig. 25 *Progressive vectors with the coordinate origin displaced laterally for clarity. Major and minor axes are oriented 230° and 320° from true north, respectively.*

UNCLASSIFIED

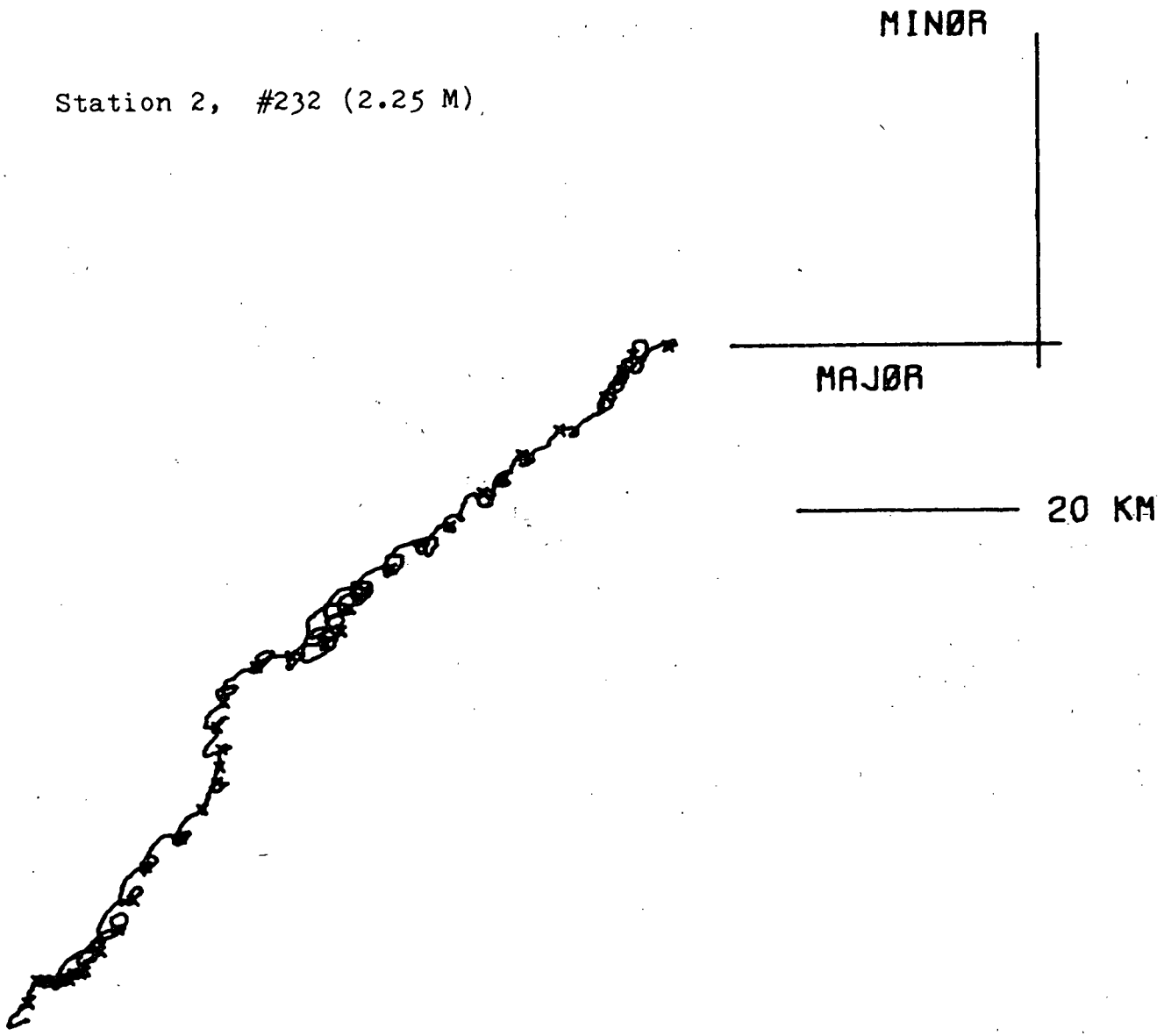

Fig. 26 As Fig. 25.

UNCLASSIFIED

Station 2, #233 (7.25 M)

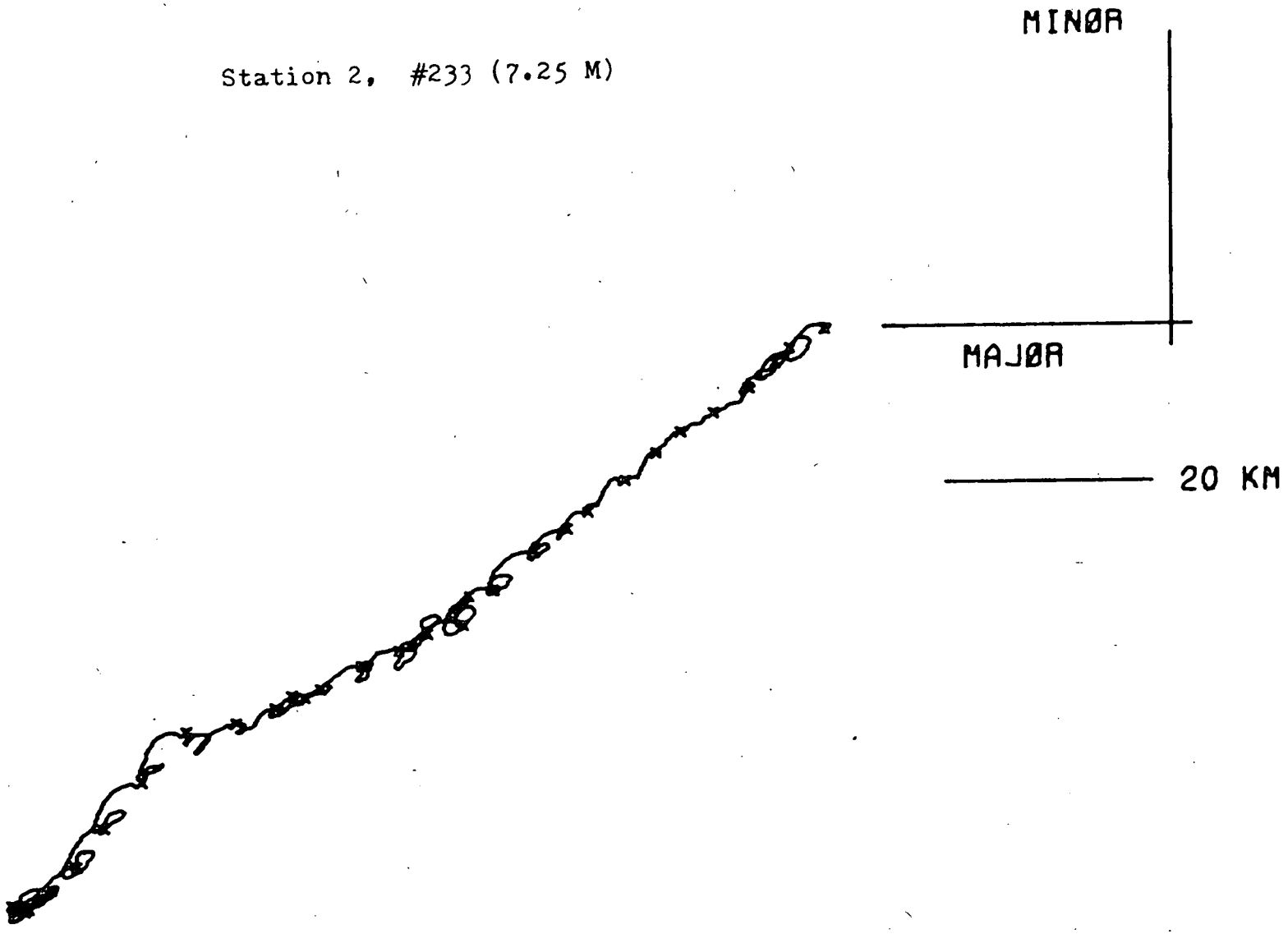

Fig. 27 As Fig. 25.

Station 2, #236 (20 M)

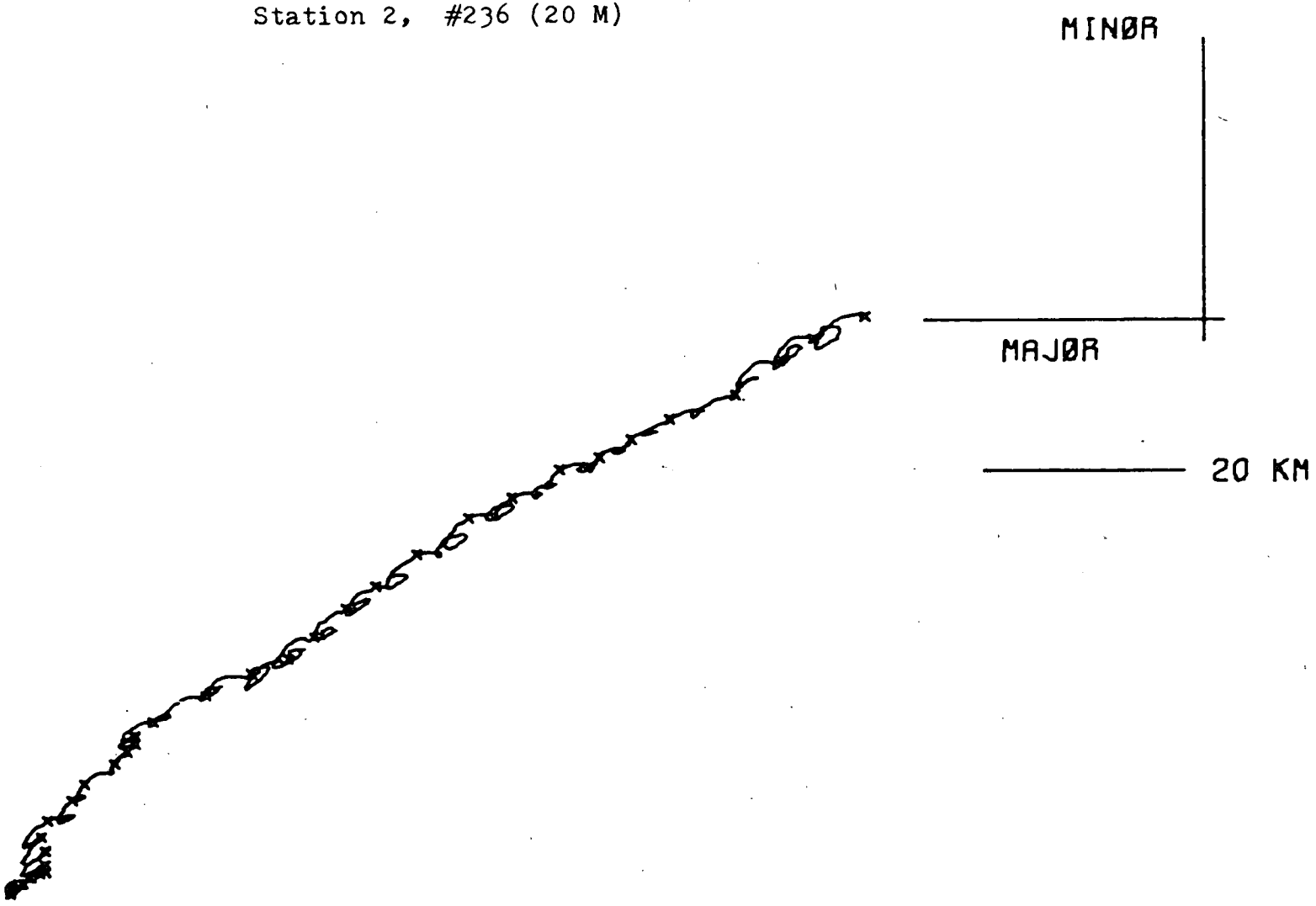

Fig. 28 *As Fig. 25.*

Station 2, #235 (50 M)

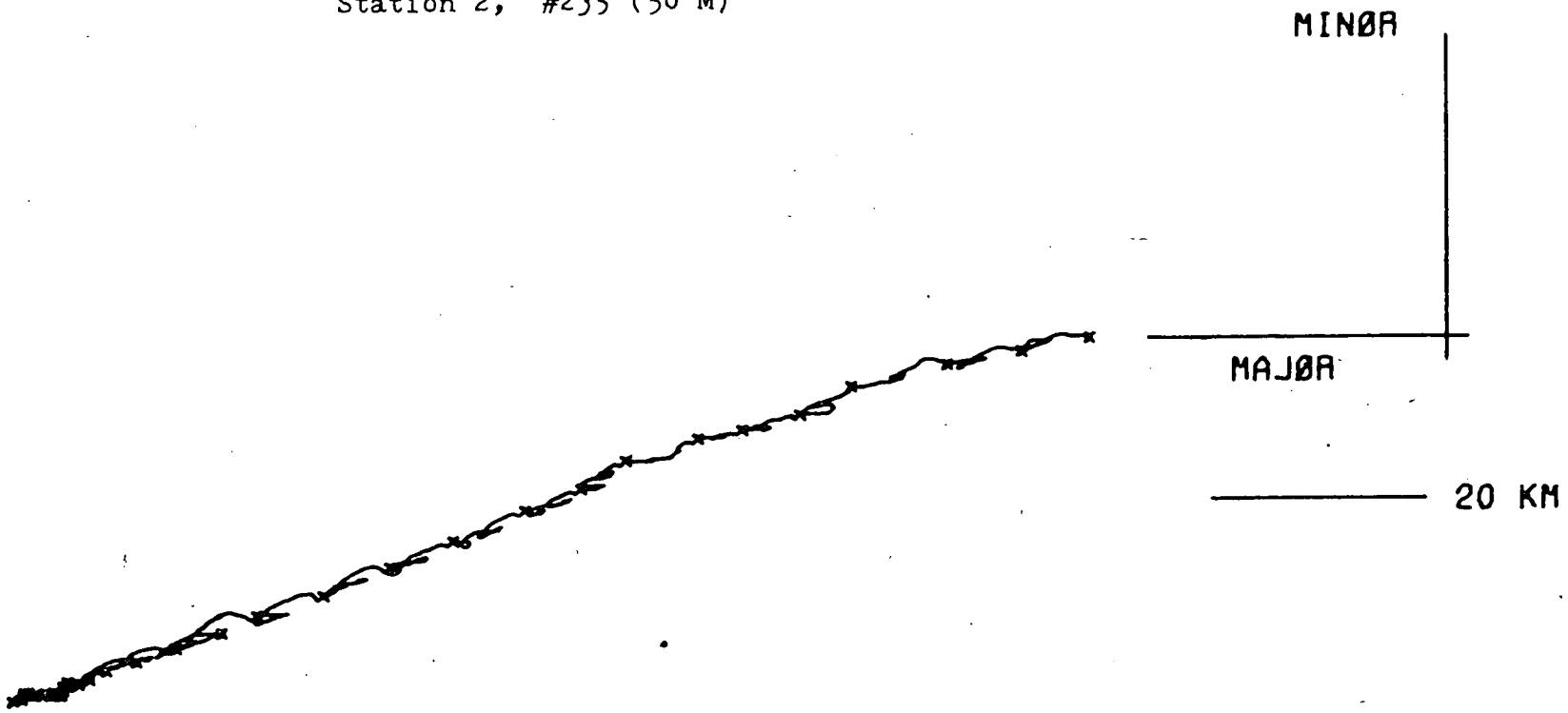

Fig. 29 *As Fig. 25.*

UNCLASSIFIED

Station 2, #234 (75 M)

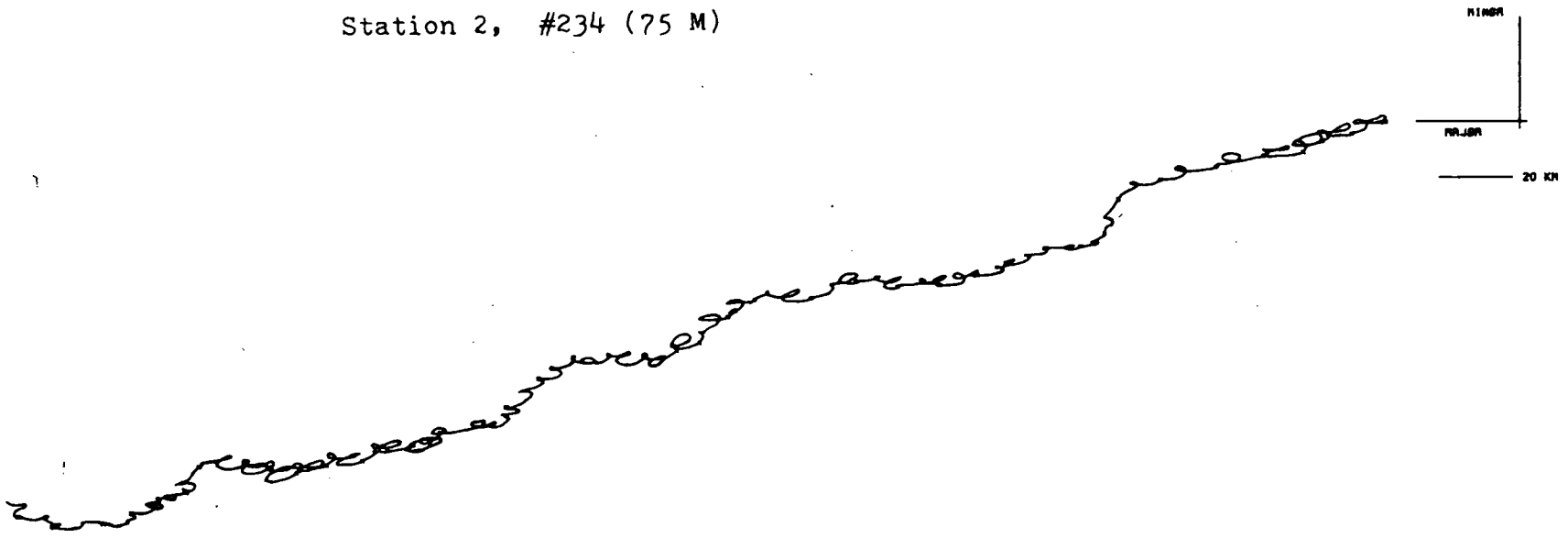

Fig. 30 *As Fig. 25.*

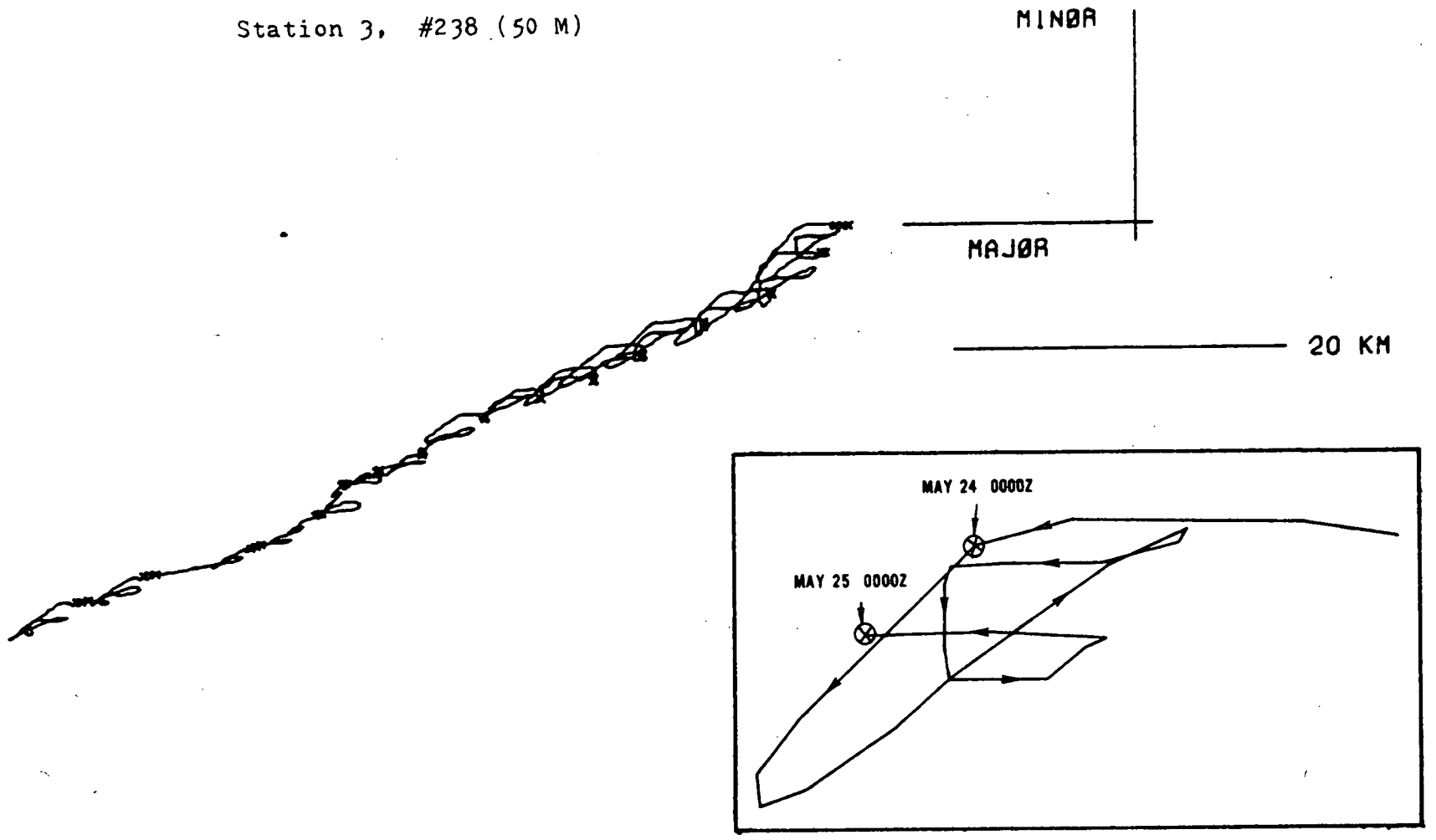

Fig. 31 *As Fig. 25. Inset, plotted from hourly velocities, shows beginning of trajectory in detail.*

UNCLASSIFIED

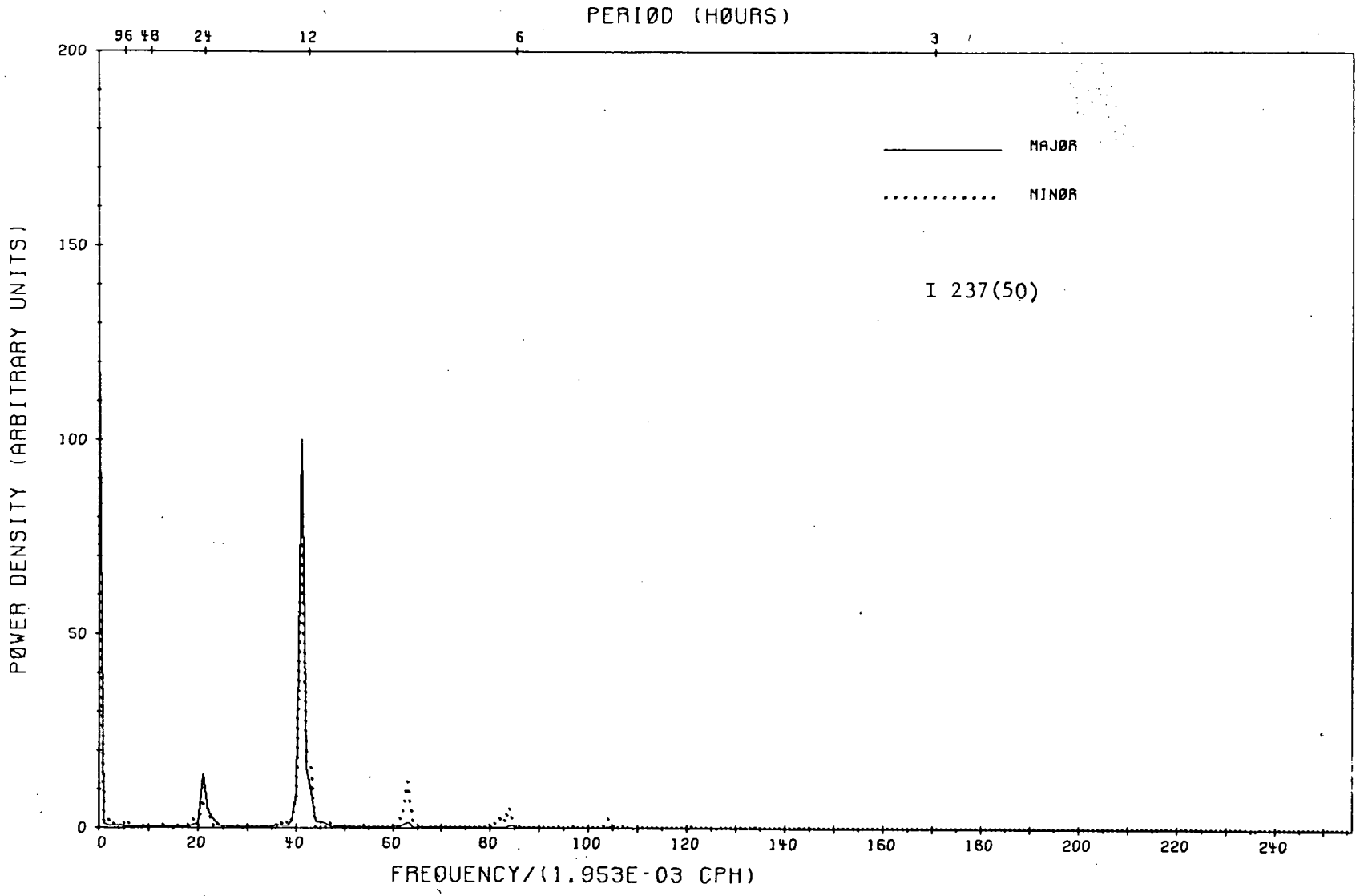

Fig. 32 *Normalized power spectra of the major and minor components of current plotted against frequency. The corresponding periods in hours are indicated at the top of graphs. I denotes Station 1 and depth in brackets. See Fig 37 for identification of oscillations.*

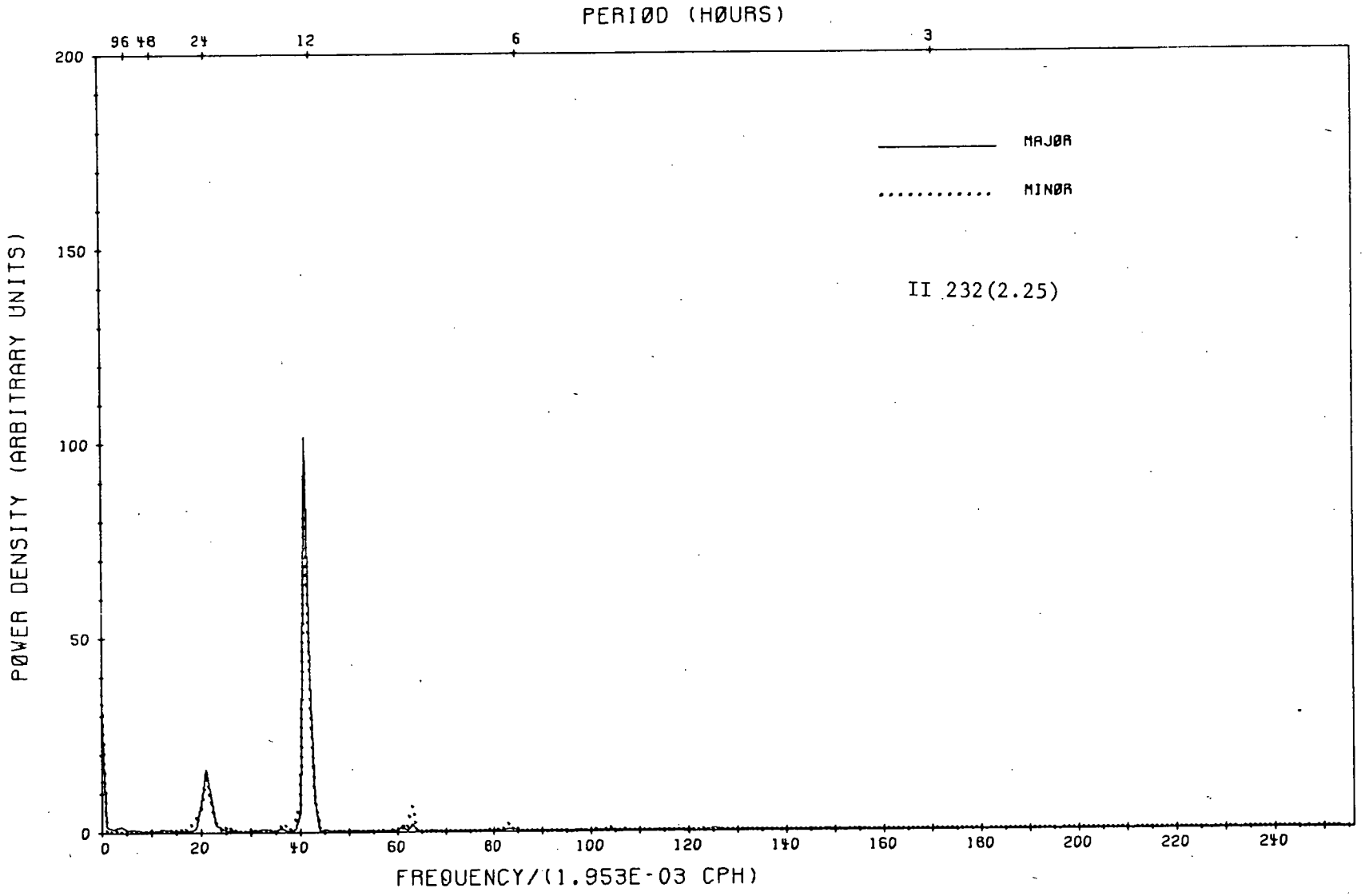

Fig. 33 *As Fig. 32. II denotes Station 2.*

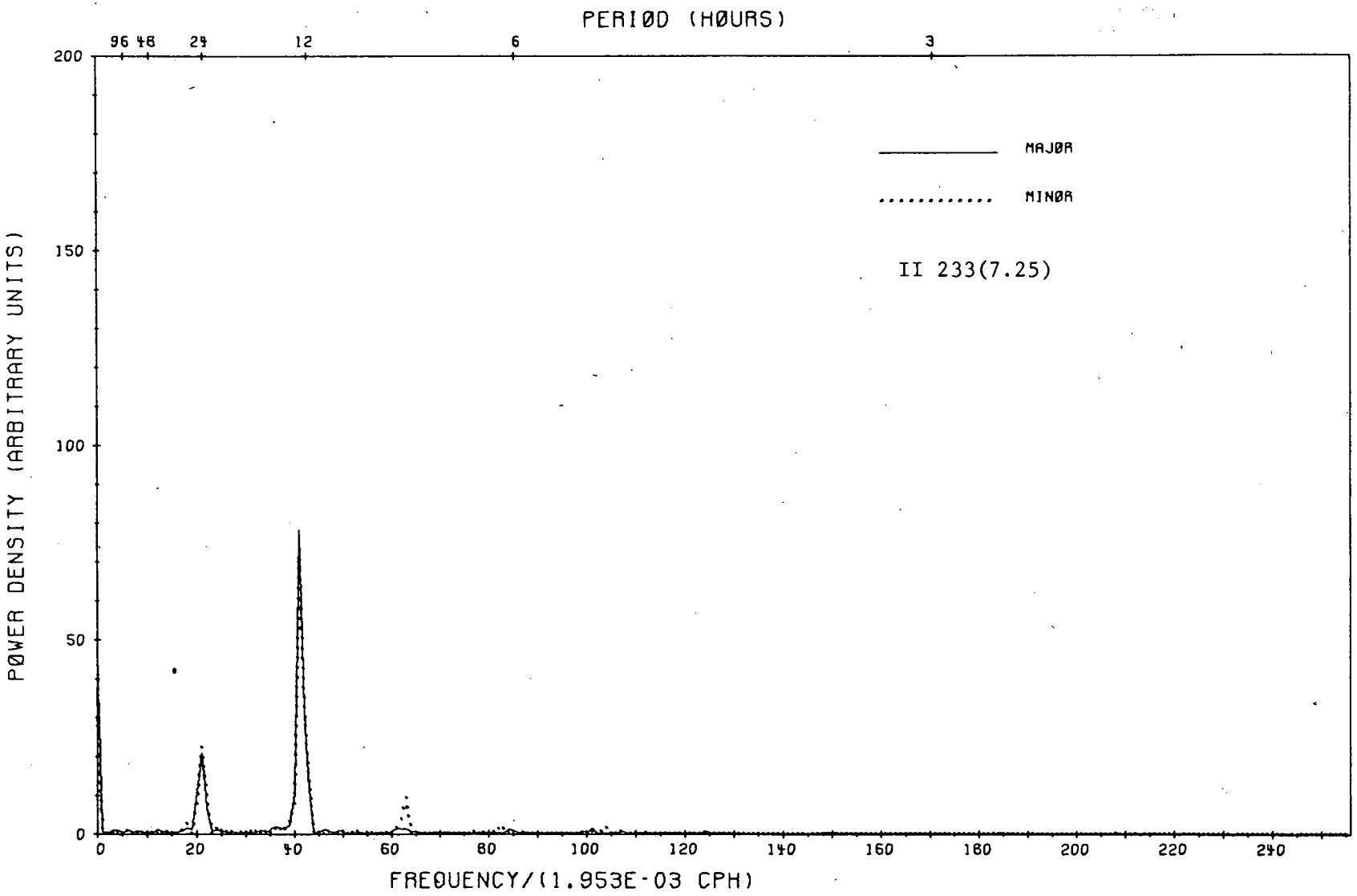

Fig. 34 *As Fig. 33.*

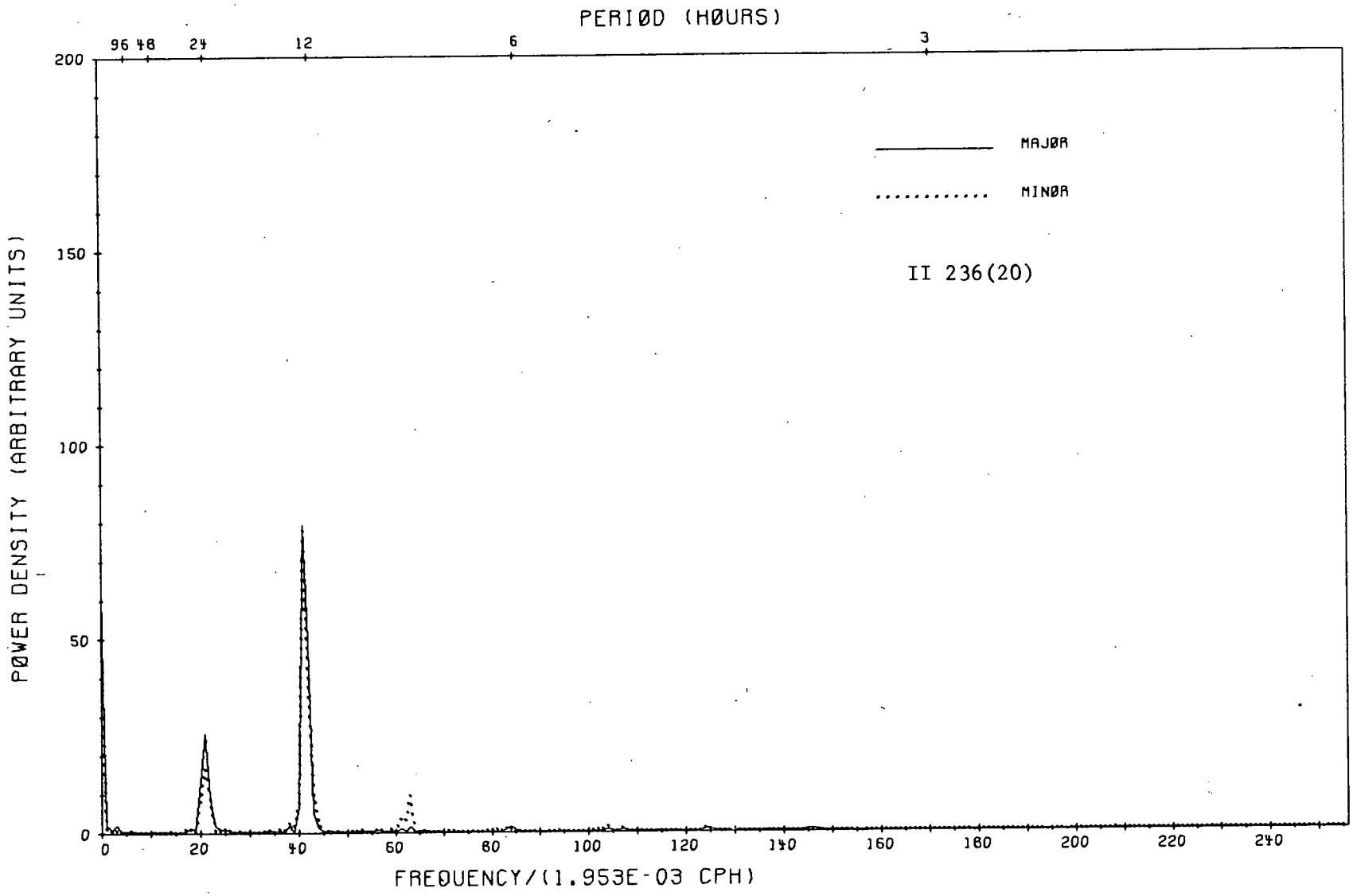

Fig. 35 As Fig. 33.

UNCLASSIFIED

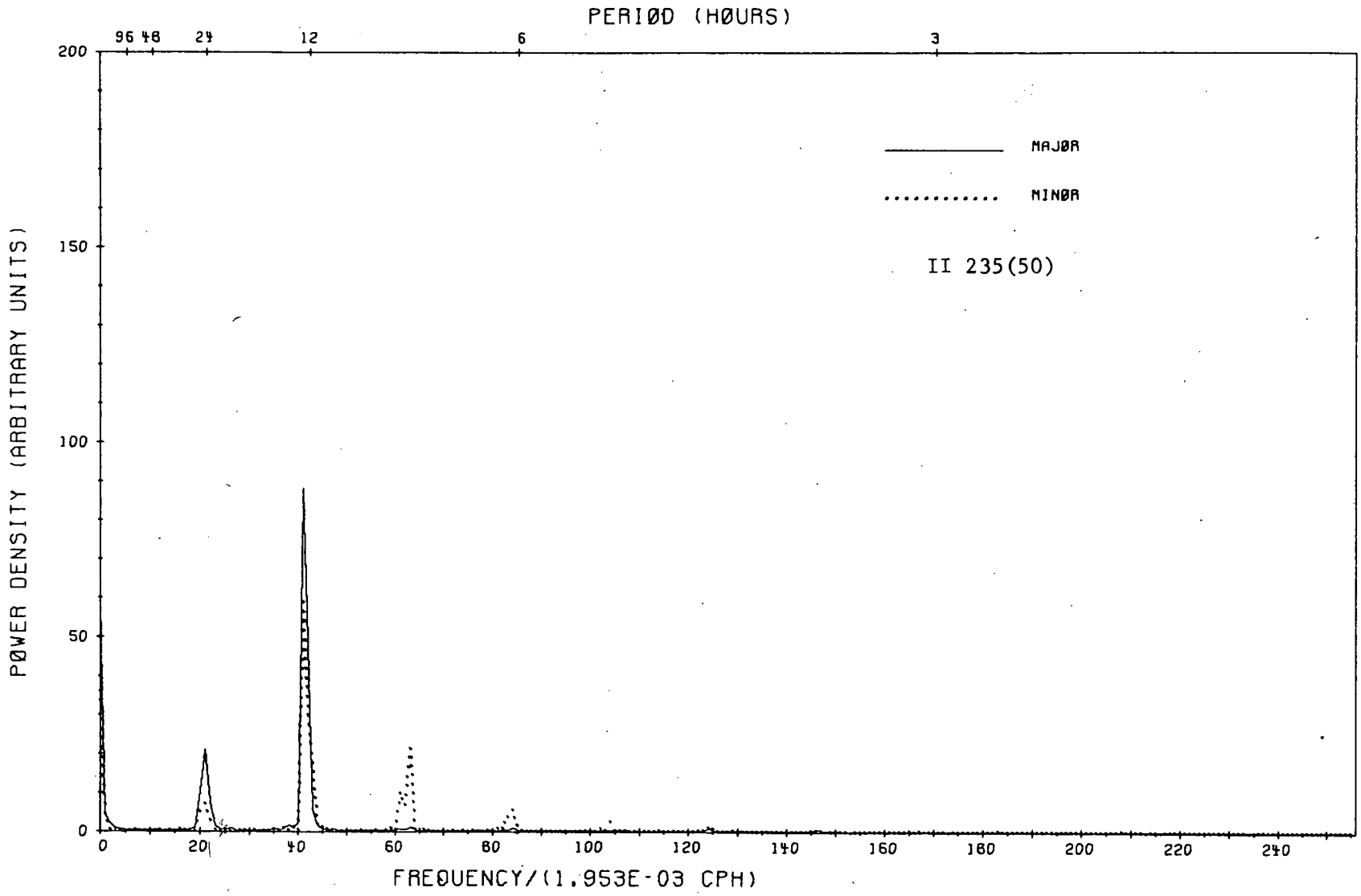

Fig. 36 *As Fig. 33.*

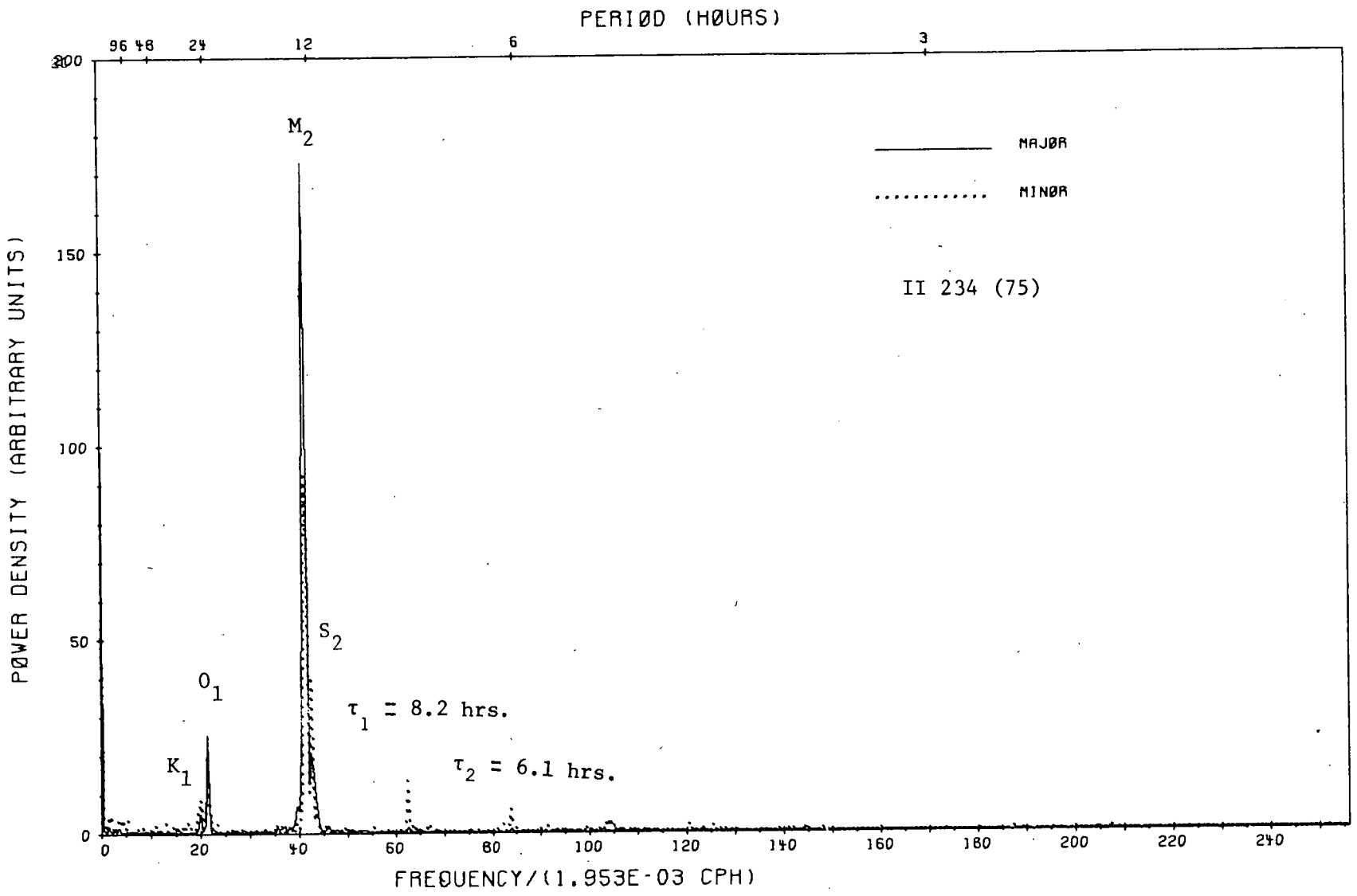

Fig. 37 *As Fig. 33. Some of the oscillations are identified.*

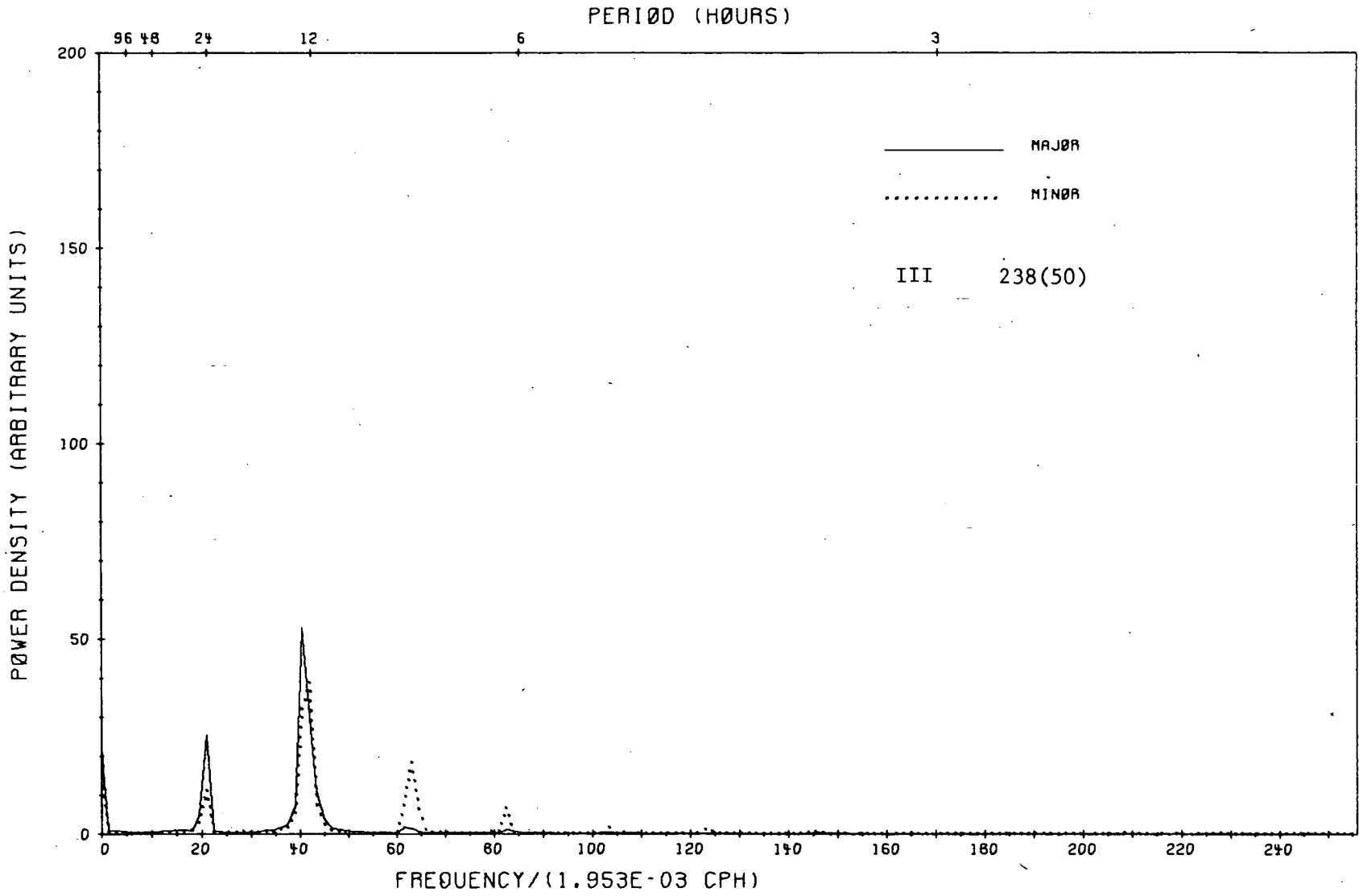

Fig. 38 *As Fig. 32. III denotes Station 3.*

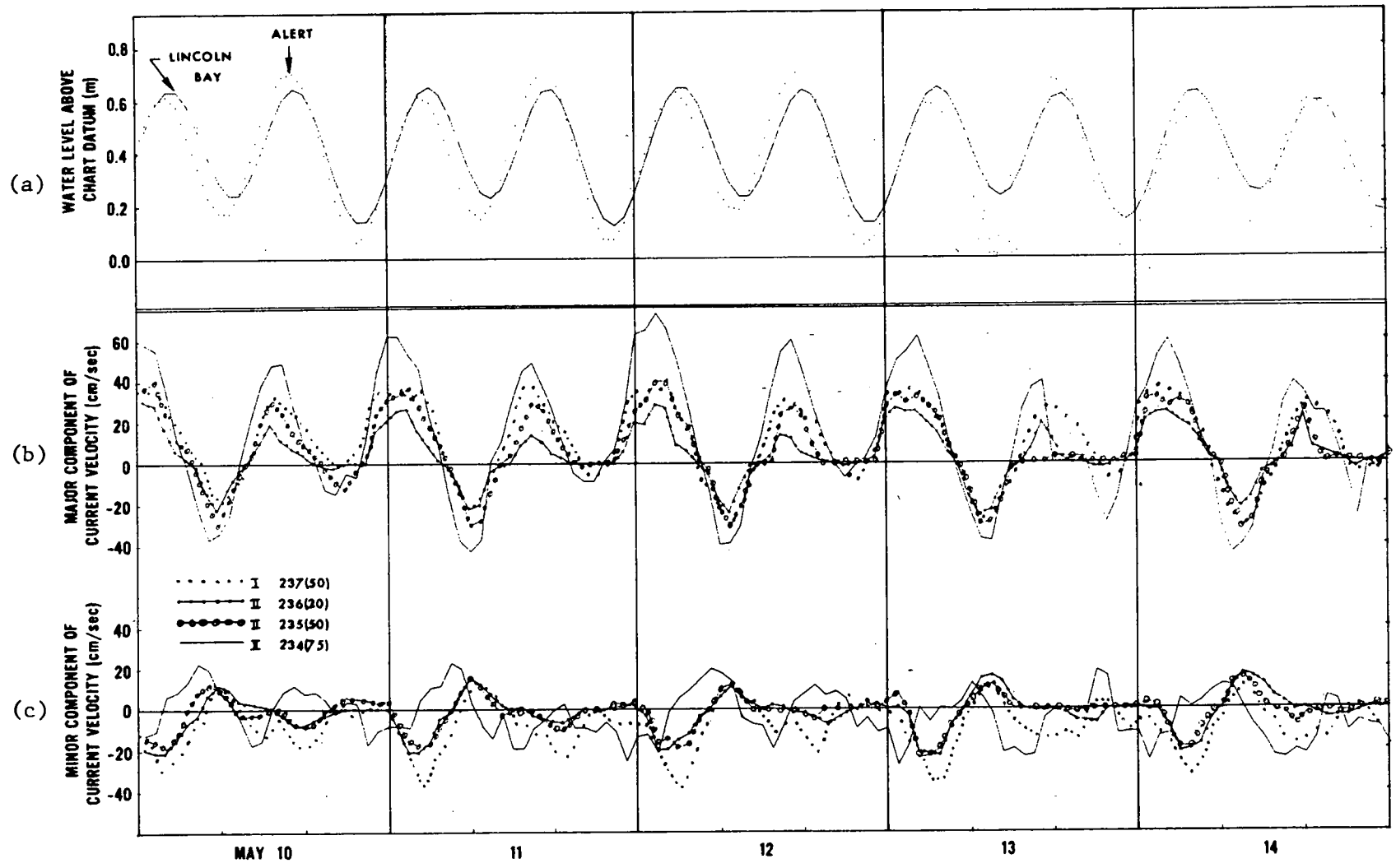

Fig. 39 *Selected sections of water levels at Alert and Lincoln Bay (a), major (b) and minor (c) components of the current for May 10-14. Stations are denoted by I, II and III.*

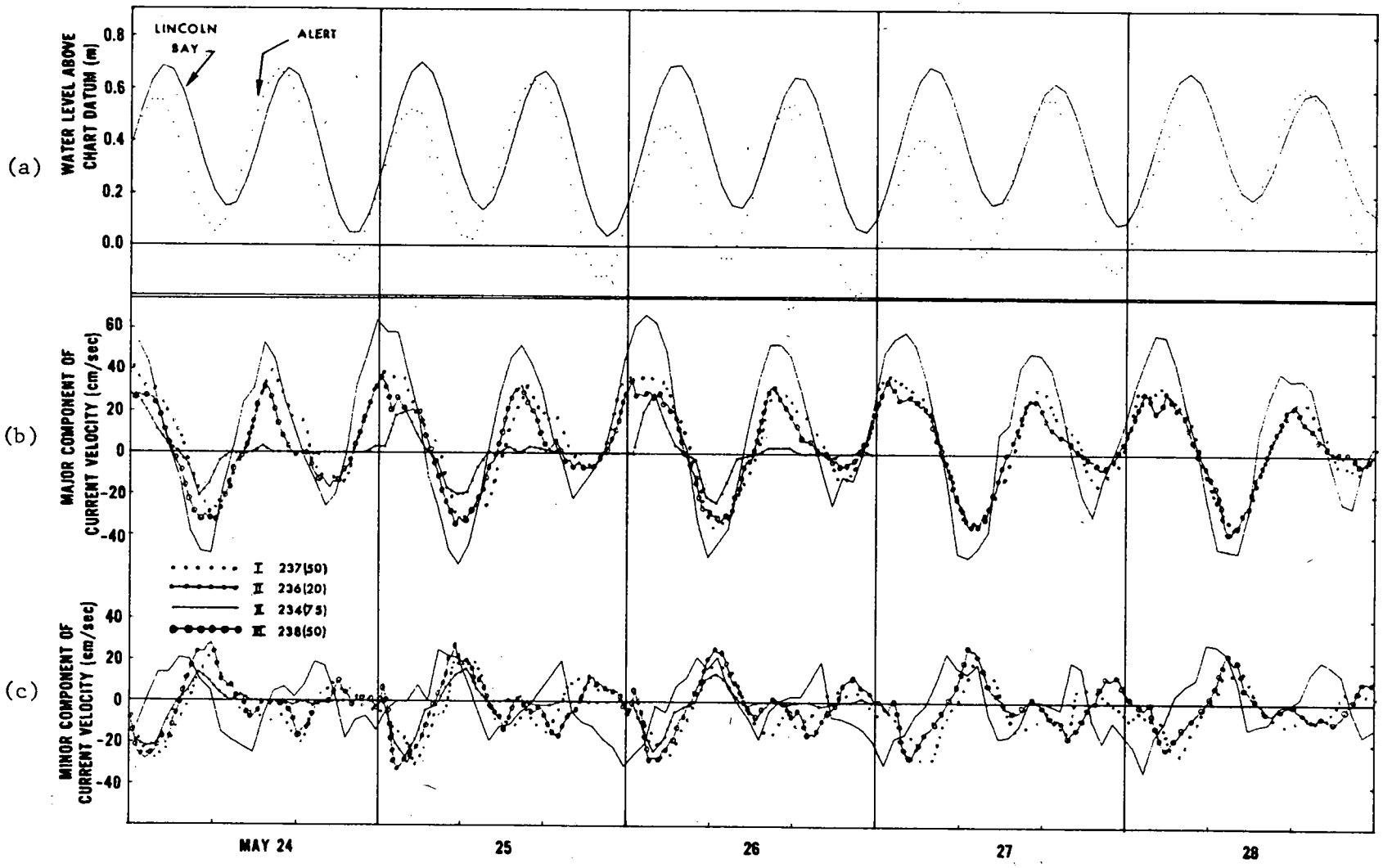

Fig. 40 As Fig. 39 for May 24-28.

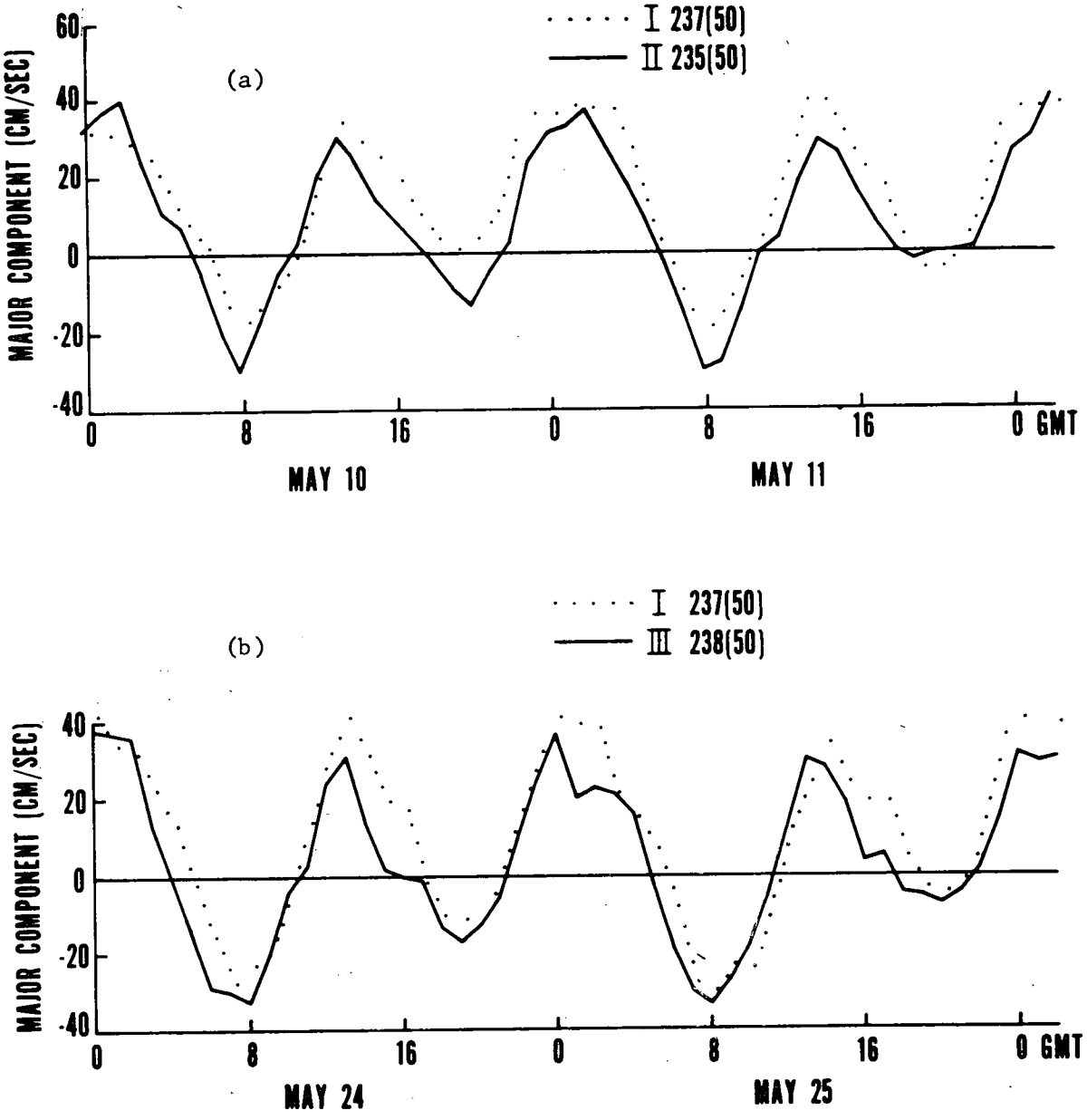

Fig. 41 *Major component of current at 50 m showing increase of speed to the right of direction of current flow.*

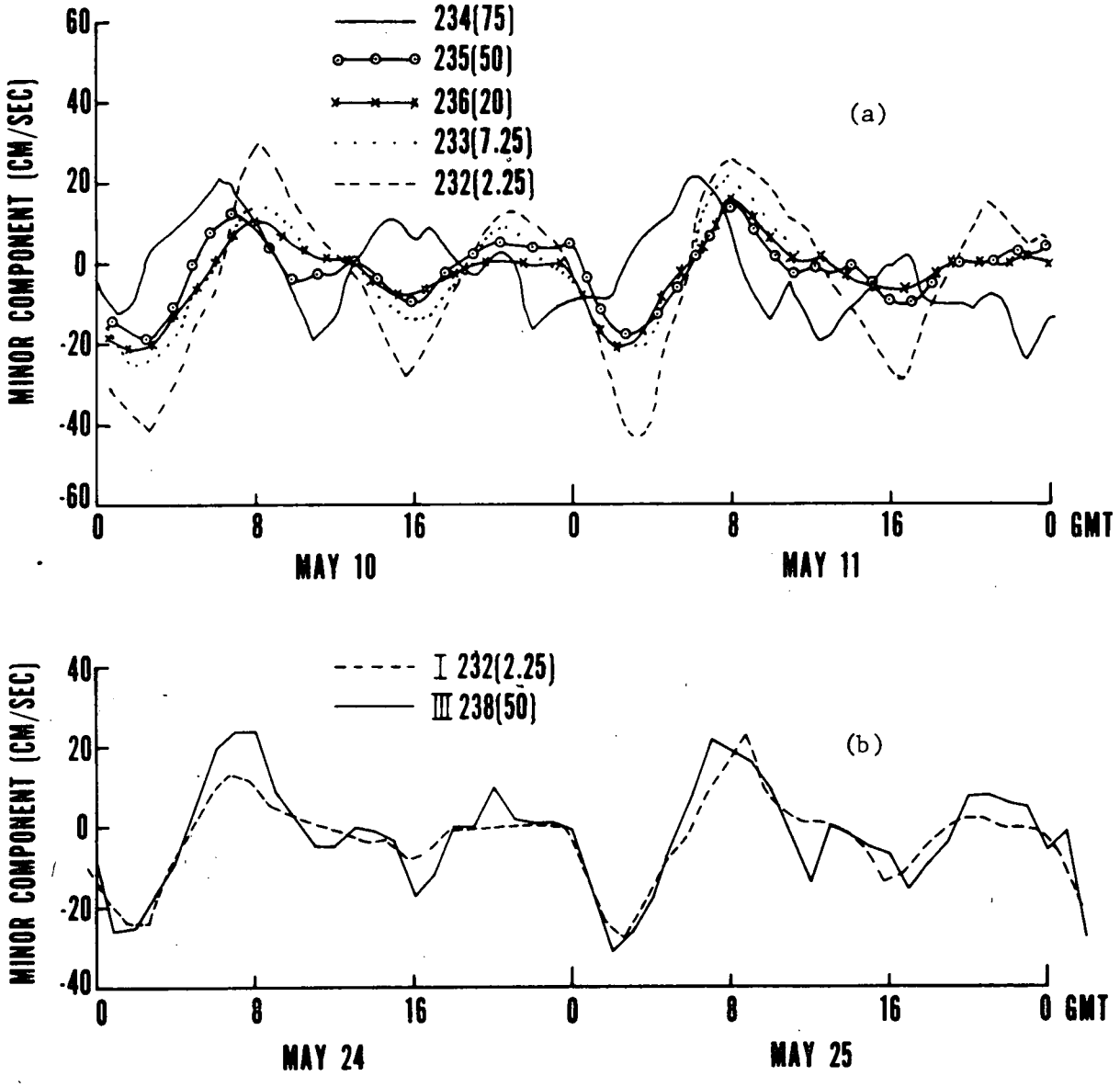

Fig. 42 *Minor component of current. (a) shows the decreasing amplitude of oscillation as depth increases to 50 m and then the phase shift at 75 m. (b) illustrates the multiple oscillations at a depth 50 m during the weaker semi-diurnal oscillations.*

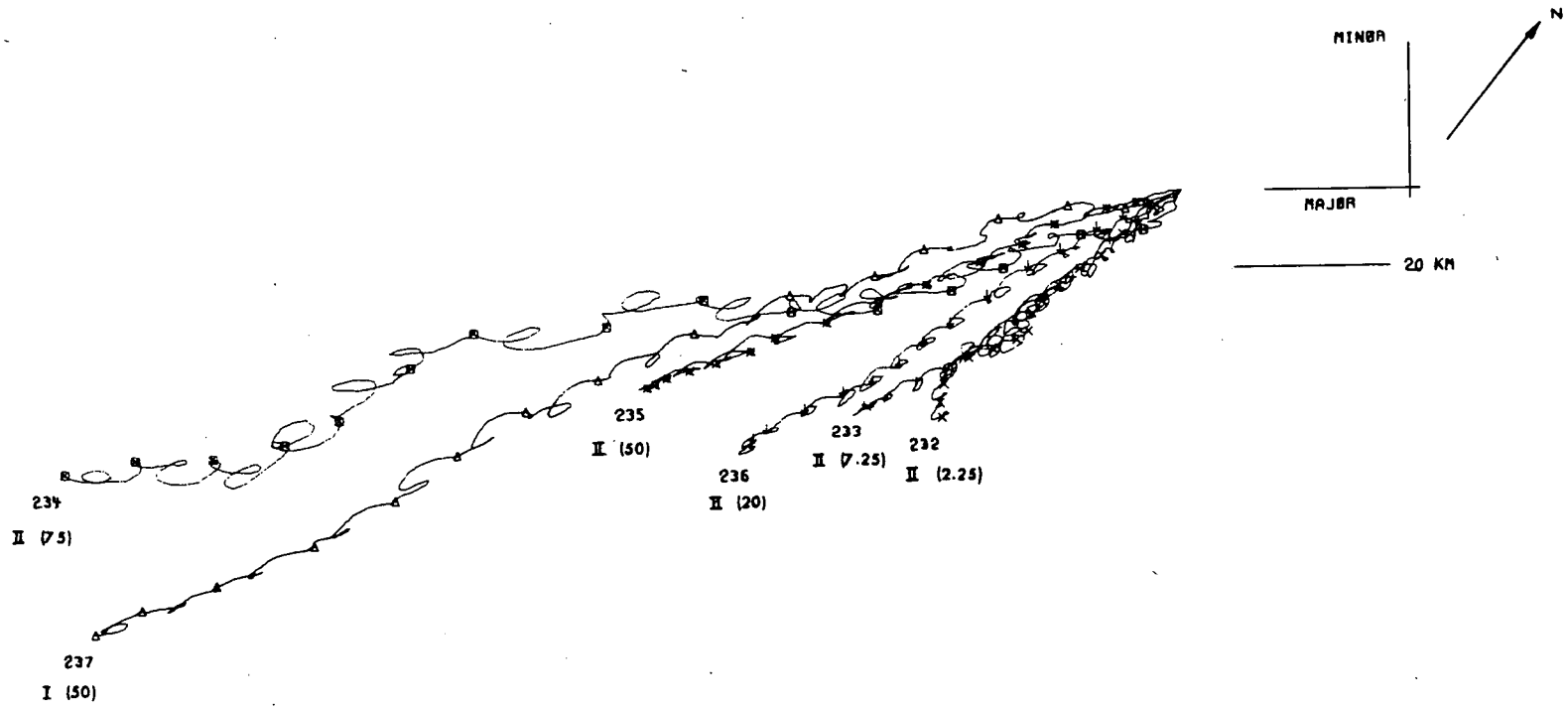

Fig. 43 *Composite current trajectories for the period May 4 - May 18. Successive marks on a curve denote 24-hour period.*

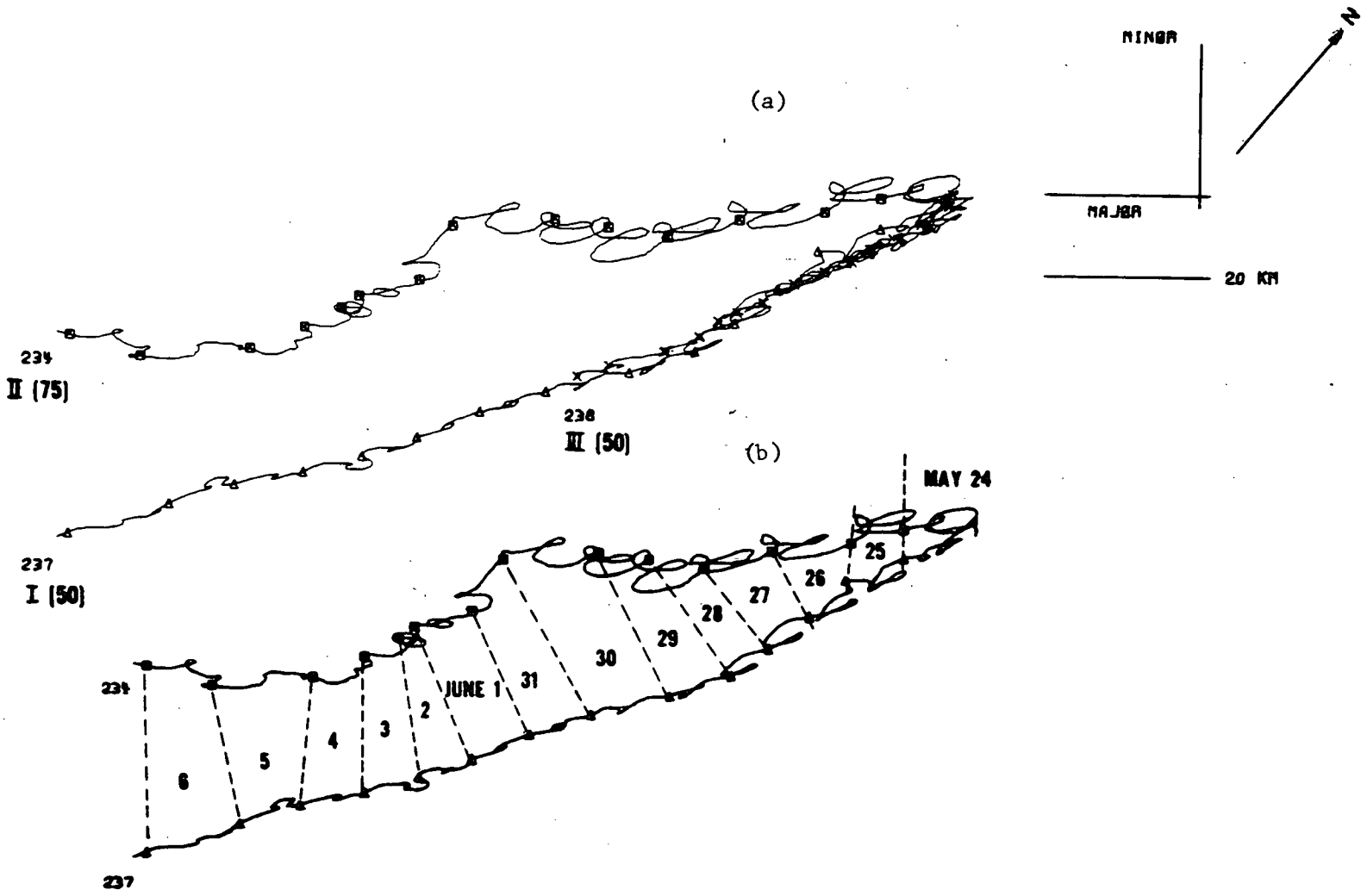

Fig. 44 *Same as Fig. 43 for the period May 24 - June 6. (b) shows the opposite rotation of two current trajectories in detail.*

UNCLASSIFIED

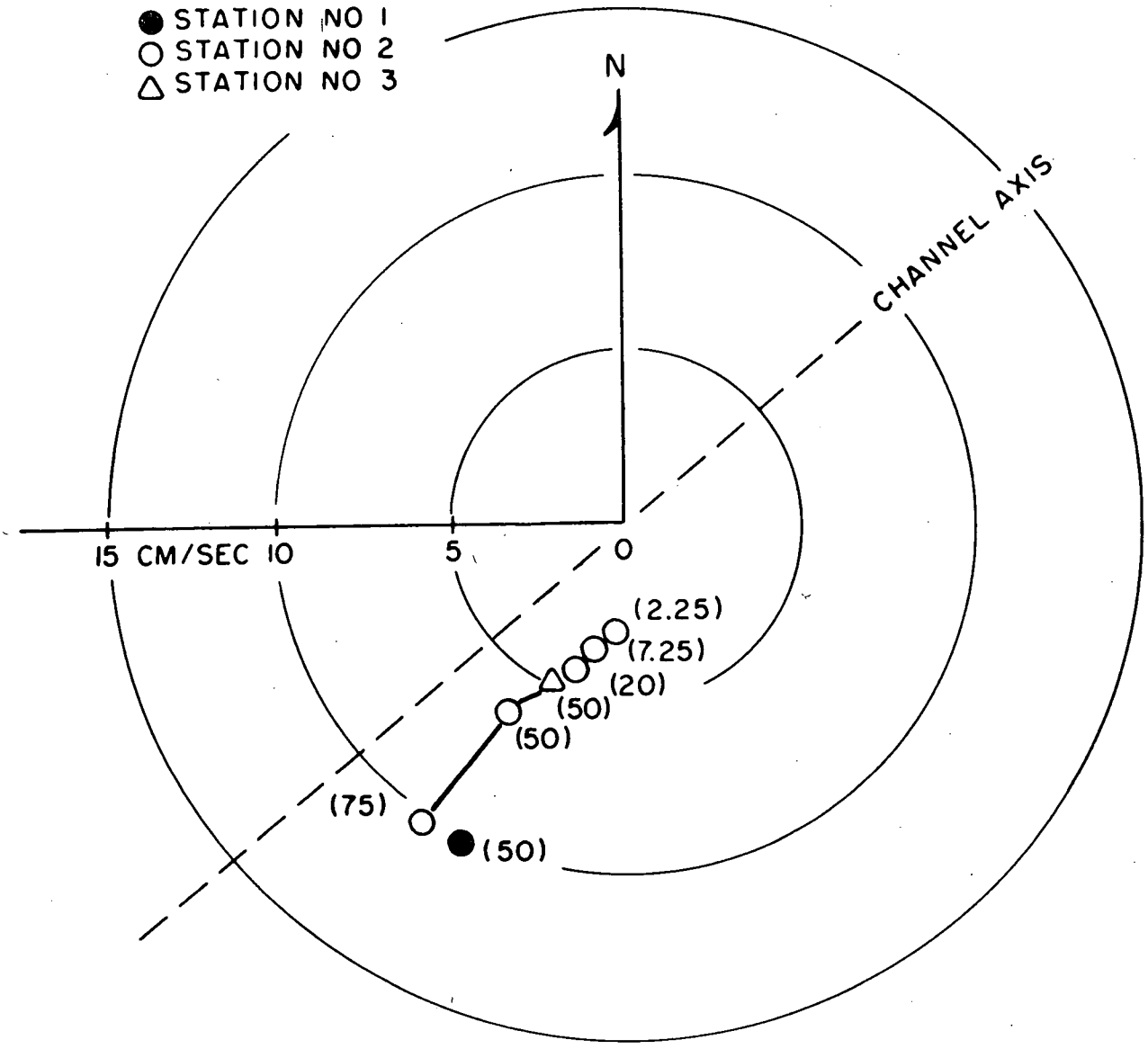

Fig. 45 Average velocity profile.

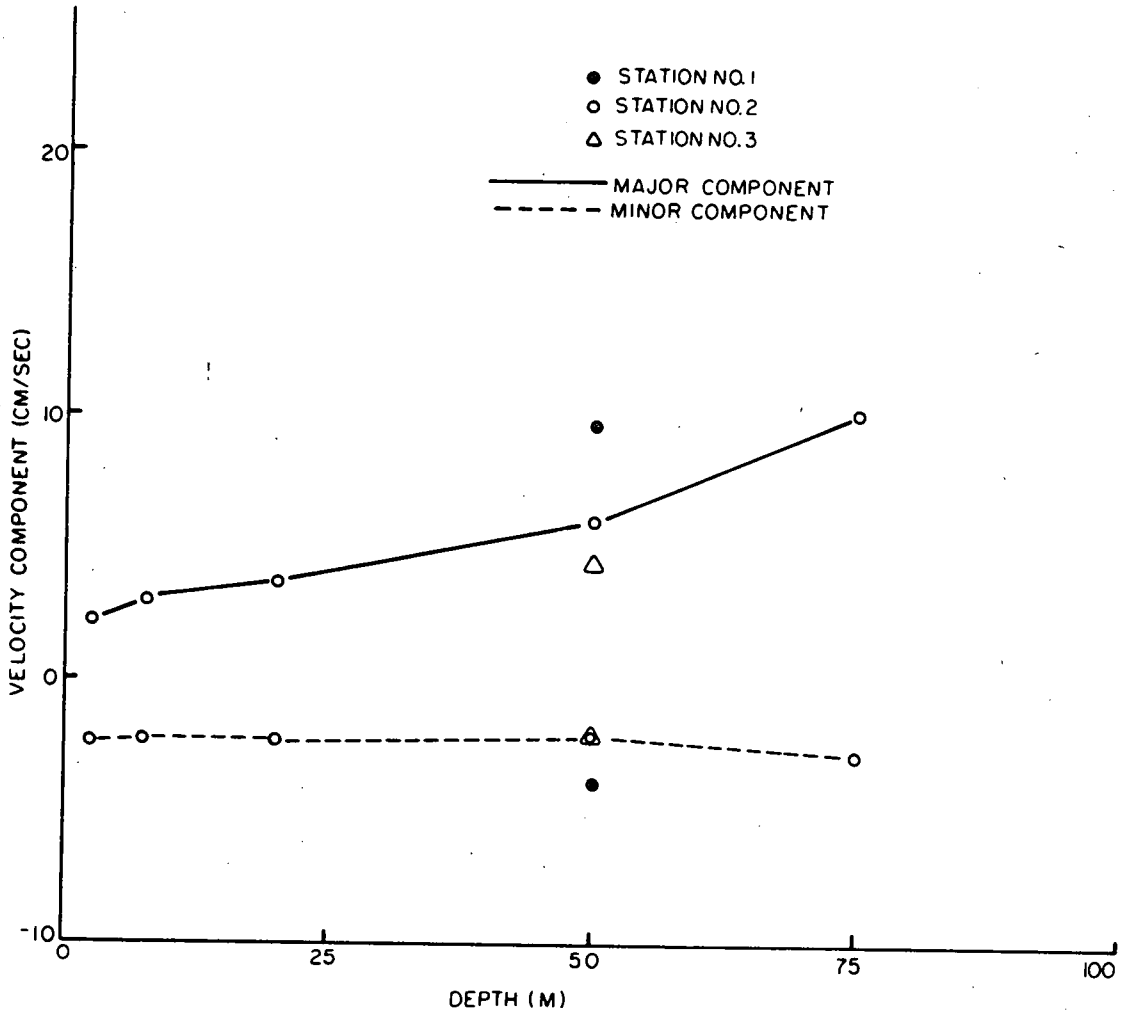

Fig. 46 Average speeds in the longitudinal and transverse directions.

4101 U 42 U
4102 U
4103 U

0201 DREO
0202 404576

UNCLASSIFIED

Security Classification

DOCUMENT CONTROL DATA – R & D

(Security classification of title, body of abstract and indexing annotation must be entered when the overall document is classified)

1. ORIGINATING ACTIVITY

0204 4a Defence Research Establishment Ottawa,
b National Defence Headquarters, Ottawa, Ontario
Ottawa ONT (CAN)

2a. DOCUMENT SECURITY CLASSIFICATION
Unclassified

2b. GROUP
N/A

3. DOCUMENT TITLE

04 NEAR-SURFACE CURRENT IN ROBESON CHANNEL

4. DESCRIPTIVE NOTES (Type of report and inclusive dates)
DREO Report

5. AUTHOR(S) (Last name, first name, middle initial)

1101
CHOW, R.K.

07 CAN

6. DOCUMENT DATE
Jan 75
+6 December 18 1974

7a. TOTAL NO. OF PAGES
0901 63 67

7b. NO. OF REFS
0902 7

8a. PROJECT OR GRANT NO.
35 D-97-67-05

9a. ORIGINATOR'S DOCUMENT NUMBER(S)
0203 709

8b. CONTRACT NO.

9b. OTHER DOCUMENT NO.(S) (Any other numbers that may be assigned this document)

10. DISTRIBUTION STATEMENT
Unlimited Distribution

11. SUPPLEMENTARY NOTES

12. SPONSORING ACTIVITY

13. ABSTRACT

UNCLASSIFIED

In this report, near-surface current data in Robeson Channel are analysed and the prominent characteristics of the current are described. Comparison of the current velocity between vertical as well as lateral positions in a cross section of the channel is made. Tidal and non-tidal oscillations in the velocity components are identified and the near-surface average current profile which may be used for mass transport calculation is obtained.

DSIS
72-508

DC

UNCLASSIFIED

Security Classification

KEY WORDS

near-surface current
Robeson Channel
tidal oscillations
internal waves
mass transport
Arctic oceanography

INSTRUCTIONS

1. ORIGINATING ACTIVITY: Enter the name and address of the organization issuing the document.

2a. DOCUMENT SECURITY CLASSIFICATION: Enter the overall security classification of the document including special warning terms whenever applicable.

2b. GROUP: Enter security reclassification group number. The three groups are defined in Appendix 'M' of the DRB Security Regulations.

3. DOCUMENT TITLE: Enter the complete document title in all capital letters. Titles in all cases should be unclassified. If a sufficiently descriptive title cannot be selected without classification, show title classification with the usual one-capital-letter abbreviation in parentheses immediately following the title.

4. DESCRIPTIVE NOTES: Enter the category of document, e.g. technical report, technical note or technical letter. If appropriate, enter the type of document, e.g. interim, progress, summary, annual or final. Give the inclusive dates when a specific reporting period is covered.

5. AUTHOR(S): Enter the name(s) of author(s) as shown on or in the document. Enter last name, first name, middle initial. If military, show rank. The name of the principal author is an absolute minimum requirement.

6. DOCUMENT DATE: Enter the date (month, year) of Establishment approval for publication of the document.

7a. TOTAL NUMBER OF PAGES: The total page count should follow normal pagination procedures, i.e., enter the number of pages containing information.

7b. NUMBER OF REFERENCES: Enter the total number of references cited in the document.

8a. PROJECT OR GRANT NUMBER: If appropriate, enter the applicable research and development project or grant number under which the document was written.

8b. CONTRACT NUMBER: If appropriate, enter the applicable number under which the document was written.

9a. ORIGINATOR'S DOCUMENT NUMBER(S): Enter the official document number by which the document will be identified and controlled by the originating activity. This number must be unique to this document.

9b. OTHER DOCUMENT NUMBER(S): If the document has been assigned any other document numbers (either by the originator or by the sponsor), also enter this number(s).

10. DISTRIBUTION STATEMENT: Enter any limitations on further dissemination of the document, other than those imposed by security classification, using standard statements such as:

(1) "Qualified requesters may obtain copies of this document from their defence documentation center."

(2) "Announcement and dissemination of this document is not authorized without prior approval from originating activity."

11. SUPPLEMENTARY NOTES: Use for additional explanatory notes.

12. SPONSORING ACTIVITY: Enter the name of the departmental project office or laboratory sponsoring the research and development. Include address.

13. ABSTRACT: Enter an abstract giving a brief and factual summary of the document, even though it may also appear elsewhere in the body of the document itself. It is highly desirable that the abstract of classified documents be unclassified. Each paragraph of the abstract shall end with an indication of the security classification of the information in the paragraph (unless the document itself is unclassified) represented as (TS), (S), (C), (R), or (U).

The length of the abstract should be limited to 20 single-spaced standard typewritten lines; 7½ inches long.

14. KEY WORDS: Key words are technically meaningful terms or short phrases that characterize a document and could be helpful in cataloging the document. Key words should be selected so that no security classification is required. Identifiers, such as equipment model designation, trade name, military project code name, geographic location, may be used as key words but will be followed by an indication of technical context.

REPORT NO: DREO REPORT NO. 709

PROJECT NO: 97-67-05

TITLE: Near-Surface Current in Robeson Channel

AUTHOR: R.K. Chow

DATED: January 1975

SECURITY GRADING: UNCLASSIFIED INITIAL DISTRIBUTION: March 1975

3 - DSIS Circ: PROGO, CRAD, Plans
Plus distribution
1 - DSIS Report Collection
1 - DREA
1 - DREP
1 - DREO for CRC via TLO
4 - DREV
1 - DREO

2 - ORAE
1 - DMOR
2 - CDLS/L, Attn: CDR
2 - CDLS/W, Attn: CDR
3 - CDLS/W
1 - RCN/LO, NAVAIRDEVCEN
3 - NRC/CB Library, Mr. Wolchuk
1 - CRRD/DGMDP
1 - SA/VCDS
5 - CEM
1 - DMCS
1 - DMFR
1 - DAASE 4
2 - CMO
1 - DMRS

Via CNDA
4 - Commander Maritime Command
1 - COS OPS
1 - SSO, Eval and Requirements
1 - MC/ORB
1 - OSD
1 - CFMWS
1 - Weapons School, CFB Halifax
3 - Maritime Headquarters Pacific
1 - SSO Op Rsch
1 - Operations & Weapons Div. Fleet School
1 - MP & EU

OTHER CANADIAN

1 - Dr. E.R. Pounder, Dept. of Physics
McGill University, Montreal, Quebec
1 - Pacific Environmental Inst.
1 - Energy, Mines & Resources, Mines Branch
1 - Library, Bedford Institute of Oceanography
1 - National Museum of Canada
1 - Great Lakes Institute, Univ. of Toronto
1 - CISTI
1 - National Library

BRITAIN
MINISTRY OF DEFENCE
2 - DRIC
Plus distribution
2 - Admiralty Research Lab. Teddington
2 - Admiralty Underwater Weapons Est.
1 - Asst. Proj. Officer for Research
IEP-ABCA-2
2 - Director of Res. Underwater, London

BRITAIN cont
1 - Director of Naval Ops. Studies London
1 - Director General Weapons Naval, Bath
1 - The Captain, HMS Vernon, Portsmouth
1 - Deputy Chief Scientist RAF London
1 - Royal Aircraft Establishment, Farnborough

BRITAIN DIRECT

1 - Royal Military College of Science
1 - National Physical Lab., Teddington
1 - National Institute of Oceanography
Wormley Near Godalming, Surrey, England

UNITED STATES

3 - DDC
Plus
4 - Naval Res. Lab., Washington, D.C.
Codes 2620, 8000, 8100, 8105
1 - Underwater Sound Ref. Div. NRL Orlando
2 - Naval Underwater Systems Center
New London, Conn
1 - Naval Undersea Center, San Diego
1 - Director, Arctic Submarine Lab. Code 90
Naval Undersea Center, San Diego, Calif
1 - USN Post Graduate School, Monterey, Calif
1 - USN Oceanographic Office, Suitland, Md.
Codes 011, 6000, 6100, 6200, 6130
1 - Office of Naval Research Washington
1 - Librarian, Naval Arctic Research Lab.
1 - Marine Physics Lab., Scripps Inst. of
Oceanography, San Diego, Calif
1 - Woods Hole Oceanographic Institution
1 - Chief of Naval Operations, Washington
1 - Asst. Sec. of the Navy (R&D)
Special Asst. for ASW, The Pentagon
1 - Center for Naval Analysis, Rosslyn, Va
1 - Inst. of Defence Analysis
1 - Weapons Systems Evaluation Group Dept of Def.
1 - Palisades SOFAR Station, APO NY 09560
1 - Oceanographer of the Navy, Alexandria Va Code N7

Via IEP-ABCA-2

3 - Lt. Cdr. A.A. Charrette, Project Officer
IEP-ABCA-2, Office of Chief of Naval Ops
Code 981G, Assistant Undersea Warfare
Development Division OP-71
Pentagon, Washington, 20350

3 - SENIOR STANDARDIZATION REP. US ARMY
Plus
2 - Air Force Systems Command
1 - Office of Foreign Disclosure Policy
1 - University Library, Maxwell AFB